**Western and
Central Pacific
Fisheries
Commission**

**SCIENTIFIC COMMITTEE
THIRTEENTH REGULAR SESSION**

**Rarotonga, Cook Islands
9 – 17 August 2017**

**Impacts of Recent High Catches of Skipjack on Fisheries on the Margins of the WCPFC
Convention Area**

**WCPFC-SC13-2017/ SA-WP-07
Rev1 (14 August 2017)**

**Inna Senina[1], Patrick Lehodey[1], Hidetada Kiyofuji[2], Masachika Masujima[2],
John Hampton[3], Neville Smith[3] and Peter Williams[3]**

[1] Marine Ecosystems Department, CLS, 11 rue Hermes, 31520 Ramonville St Agne, France
[2] National Research Institute of Far Seas Fisheries, 5-7-1 Orido, Shimizu, Shizuoka, 424-8611 Japan
[3] Secretariat of the Pacific Community, B.P. D5, 98848 Noumea Cedex, New Caledonia

Table of Content

Impacts of Recent High Catches of Skipjack on Fisheries on the Margins of the WCPFC Convention Area

Inna Senina[1], Patrick Lehodey[1], Hidetada Kiyofuji[2], Masachika Masujima[2], John Hampton[3], Neville Smith[3] and Peter Williams[3]

1 Marine Ecosystems Department, CLS, 11 rue Hermes, 31520 Ramonville St Agne, France

2 National Research Institute of Far Seas Fisheries, 5-7-1 Orido, Shimizu, Shizuoka, 424-8611 Japan

3 Secretariat of the Pacific Community, B.P. D5, 98848 Noumea Cedex, New Caledonia

----

1. Executive summary

- Since several years, there is raising concern that high purse seine catches in the equatorial region may be causing a range contraction of WCPO skipjack tuna, thus reducing skipjack tuna availability to fisheries in higher latitudes, e.g., the domestic and off-shore Japanese boats fishing seasonally in the sub-tropical and temperate home waters. Alternatively, change in environmental conditions may also generate variability in tuna recruitment, movement and catch.

- The northwest Pacific region is strongly influenced by mesoscale activity associated to the warm Kuroshio current and its extension east off Japan where it encounters the cold Oyashio current. Kuroshio extension has been shown to shift between extended and contracted regimes at interannual time scale. A change from elongated to contracted regime, characterized with less energetic conditions, was described following a transition period in 2005-2006. The contracted regime changed to an elongated regime in 2010 and since then remained in neutral conditions.

- Recent progress in application of SEAPODYM to skipjack included new environmental forcing, revision of fishing data set and parameter optimisation including conventional tagging data in addition to fishing data. This report provides the results on simulations conducted with this new reference configuration at coarse and high resolutions to test the strength of connectivity between adjacent and distant regions, and to measure the impact of equatorial purse seine fisheries on Japanese domestic fisheries.

- The new reference run at coarse resolution shows improved fit to data and realistic parameterization of biological parameters (thermal habitat, movement, oxygen tolerance, vertical habitat, spawning conditions) in good agreement with current knowledge. Predicted skipjack density is distributed mostly in the warmpool. Variability in recruitment and adult distribution due to ENSO are well predicted.

- Total stock estimates in WCPO are close between SEAPODYM and Multifan-CL, i.e. 3.4Mt of adult and about 4Mt of total biomass in 2010, but with a discrepancy in the north west Pacific region, where MULTIFAN-CL skipjack biomass estimate is much higher and more variable than SEAPODYM estimate. This does not prevent SEAPODYM to correctly predict the catch of the subtropical Japanese pole-and line north of 20° N based on the observed effort. On the other hand SEAPODYM predicts higher biomass in the two core tropical regions known to be the main fishing grounds for skipjack.

- The average fishing impact at basin scale reach 20-25% of reduction in spawning biomass by the end of 2010, buts approaching 50 % in the most intensively exploited region north of Papua New Guinea.

- After dowsncaling on high resolution configuration, a very good match is observed between high catch and high density of (exploitable) skipjack in the equatorial purse seine fishing ground including the Solomon Is. and Papua New Guinea regions, and the fit is high for the Japanese subtropical pole and line fishery as well.

- Connectivity study is conducted between regions proposed by Kiyofuji (WCPFC SC12) with both coarse and high resolution configurations. There are only small differences between the two simulations, excepted in region 7 suggesting a strong sensitivity to mesoscale circulation in this region.

- In region 1 (East off Taiwan, Okinawa Is.) adult biomass would be supported by recruitment in its own area (~30-35%), then by recruitment in the region 3 (~24- 38%), region 6 (~10-25%), region 7 (~5-13%) and 2 (~5-10%). Region 1 is well connected to regions 3 and 6 for adult exchanges (movements).

- After a tendency to decrease over 2006-2012, the larvae recruitment in region 1 shows an opposite increasing trend in the recent years. This signal is delayed in immature and then adult cohorts. The immature biomass shows an increase in the last year (2015) of the simulation while it is not yet appearing in the adult stock, in which the increase could be expected in 2016-17.

- In region 7 (North Central Pacific), density of recruited larvae is predicted to be lower by high-resolution simulation. Biomass of immature and adult cohorts follows the same trends with delayed effect as those observed in region 1.

- When removing equatorial purse seine fishing mortality, the increase in adult biomass and catch of regions 1 and 7 are limited (< 6% in both).

- Though the study suggests a significant connectivity between equatorial and higher latitudes, the high biomass predicted in the equatorial regions limits the impact of the equatorial purse seine fishery on the northern stock. It remains possible that an improved representation of skipjack distribution in the main equatorial fishing grounds could allow the model to predict the catch correctly with a lower biomass in tropical regions. In that case, the impact of purse seine fishing on the adjacent regions could become stronger.

- There are also some indications that interannual environmental variability could be responsible of a decrease in immature and adult stocks in the recent years while higher recruitment would have occurred very recently in concordance with favorable conditions associated to 2014-15 El Niño event. This should be analyzed when updated physical forcings will become available.

2. Background

Skipjack tuna is the most productive Pacific tuna species and the catch of this species in the western central Pacific Convention area represents almost 50% of the World tuna catch. During the recent decades, tuna fisheries have expanded their range worldwide with a continuous increase of fishing effort and fishing capacity leading to a dramatic increase of the catches. Most of the increase is due to the development of purse seine fleets. The western central Pacific Ocean (WCPO) has the largest skipjack fishery in the World. In 2015, the catch of skipjack in the WCPFC convention area was estimated to 1,827,750 mt (68% of the total catch) and the third highest recorded, nearly 180,000 mt less than the record in 2014 (2,005,647 mt) (Williams and Terawasi 2016). Most of that catch was due to the purse seine skipjack catch (1,416,453 mt ; 77.5% of total skipjack catch).

In addition to tropical purse seine fisheries (Fig. 1), there are pole-and-line skipjack fisheries either year-round in the tropical region, or seasonal in the sub-tropical and temperate home waters of Japan. Japan has two pole-and-line fleets that catch skipjack, the domestic off-shore fleet and the tropical fleet. The offshore fleet is consisting of medium-size boats fishing seasonally in the sub-tropical and temperate home waters of Japan, mainly between August to November. The tropical fleet includes large boats fishing year-round in the tropical region. There are also miscellaneous fisheries (troll, set net and gillnet) catching skipjack and other tunas and tuna like species along the coasts of Japan.

A gradual reduction in numbers of vessels has occurred in all pole-and-line fleets over the past decades (Fig 1) leading in parallel to the decrease of catches by the Japanese distant-water and offshore fleet. Most skipjack catch is taken in equatorial areas and the remainder is taken in the seasonal domestic (home-water) fishery of Japan and the domestic fisheries in Indonesia and the Philippines. Philippines and Indonesian domestic fisheries account for most of the skipjack catch in the 20–40 cm size range (Williams and Terawasi 2016).
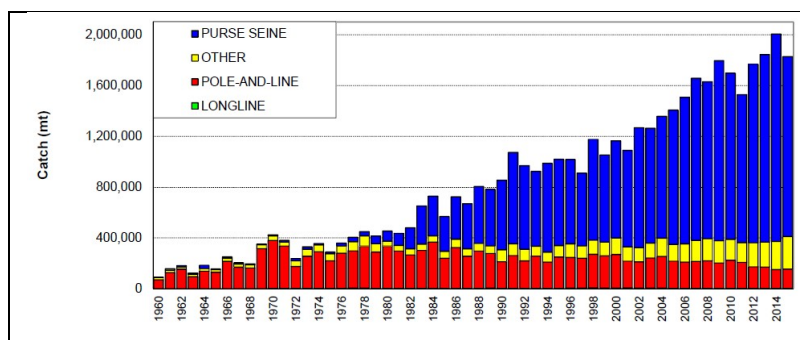

Figure 1: WCP–CA skipjack catch (mt) by gear. From Williams and Terawasi (2016).

The last scientific committee of the WCPFC (SC12) was unable to reach consensus on the description of stock status (WCPFC 2016). However, the SC noted that the stock is currently moderately exploited and fishing mortality level is sustainable, though the skipjack spawning biomass is now around the TRP (Threshold Reference Point) set to 50% of reduction in spawning biomass relatively to unfished biomass ($B_{S, F=0}$).

Since several years, there is raising concern that high catches in the equatorial region may be causing a range contraction of WCPO skipjack tuna, thus reducing skipjack tuna availability to fisheries conducted at higher latitudes than the Pacific equatorial region (WCPFC 2016; Kiyofuji 2016; Pilling et al 2016). In 2010, a first study relying on oceanographical analyses and SEAPODYM model simulations showed that different regimes in the Kurohio extension (extended

vs contracted) occuring at interannual time scale can impact the distribution, catchability and local recruitment of skipjack in Japan domestic waters. A change from elongated to contracted regime, characterized with less energetic conditions, was described following a transition period in 2005-2006 and predicted to coincide with an increase in abundance of young fish in the northern coastal Japanese fishing ground. Following this study, a « Kuroshio box » with an index based on altimetry was implemented on the AVISO website (Bessière et al. 2012) to monitor the state of the system in real time (Figure A1 in appendix). The contracted regime changed to an elongated regime in 2010 and since then remained in neutral conditions.

The model SEAPODYM also predicted a general lower abundance of adult fish in 2008 due to lower recruitment in the population. Finally, a simulation with no purse seine fishing did not demonstrate any strong interaction with the north Pacific fishing grounds. Since this study, various progresses have been achieved in SEAPODYM modeling and its application to skipjack. One major improvement is the recent addition of conventional tagging data in the maximum likelihood estimation (MLE) approach to optimize the model parameters (Senina et al. 2016). With a better definition of fishing data sets and improved physical forcings, it has been proposed during SC12 to revise this first connectivity study based on SEAPODYM. This report provides the results achieved using the recent progress in SEAPODYM skipjack modeling with additional simulations conducted to test the strength of connectivity between adjacent and distant regions and measure the impact of equatorial purse seine fisheries on Japanese domestic fisheries.

3. Methods

3.1. SEAPODYM.V3

The modeling approach of SEAPODYM has been extensively described in previous working documents of the WCPFC (Lehodey 2004; 2005; Lehodey and Senina 2009; Senina et al. 2016) and in the scientific litterature (Lehodey et al 2008, 2013; Senina et al 2008, Sibert et al 2012; Dragon et al 20). Unlike standard assessment model like MULTIFAN-CL or Stock Synthesis, SEAPODYM model equations describe fish population dynamic processes (spawning, recruitment, movement, mortality) based on environmental functional relationships with temperature, dissolved oxygen concentration and distributions of prey (micronektonic tuna forage). The model simulates tuna age-structured population dynamics with different life stages. At larvae and juvenile phases, fish drift with currents; later on they become autonomous, i.e., in addition to the currents velocities their movement has additional component linked to their size and the habitat quality, as well as oceanic currents. The model takes into account fishing and predicts total catch and size frequencies of catch by fishery. The spatial dynamics, relying on advection-diffusion-reaction equations is fully-explicit, meaning that density of fish cohorts and catch are computed in each cell of a grid defined for the model domain, with spatial resolution typically between 2° and 0.25°. The Maximum Likelihood Estimation approach developed for SEAPODYM takes advantage of this spatially explicit representation by using the numerous (>> 100,000) catch/effort and length frequencies of catch data available at these resolutions. The recent progress of the last few years led to the release of a new version (V3) with the following key major changes:

- Implementation of conventional tagging data in the Maximum likelihood Estimation approach to improve the estimate of habitats and movements parameters. The method is presented in Senina et al. (2016). Only fully reliable information from tagging experiment is used, i.e., release and recapture position and size at release. Tagging data is not use to estimate natural mortality.

- Implementation of alternative approach to account for fishing mortality and to predict catch without fishing effort, i.e. based on observed catch and model biomass. This apporach is

particularly useful when there is no fishing effort data or the fishing effort is not reliable or too noisy.

- Revision of the spawning habitat with prey and predator functions defined separately (instead of using the prey-predator ratio as in previous version).

- One additional parameter associated to each functional group of prey providing more flexibility in the representation of vertical behavior and access to tuna forage.

This new version of SEAPODYM (v3) has been applied to Pacific skipjack population and fisheries for the period 1980-2010 and the results presented to the last meeting of the WCPFC scientific committee (Senina et al 2016). The optimization was achieved using a basin scale configuration at a resolution of 2° x month with a revised fishing dataset provided by SPC and IATTC representing all the main historical skipjack fisheries (Table A1; Figure 2) and a set of physical variables produced with a coupled physical-biogeochemical model NEMO-PISCES driven by the atmospheric reanalysis (~observations) INTERIM at a 2°x month reoslution.
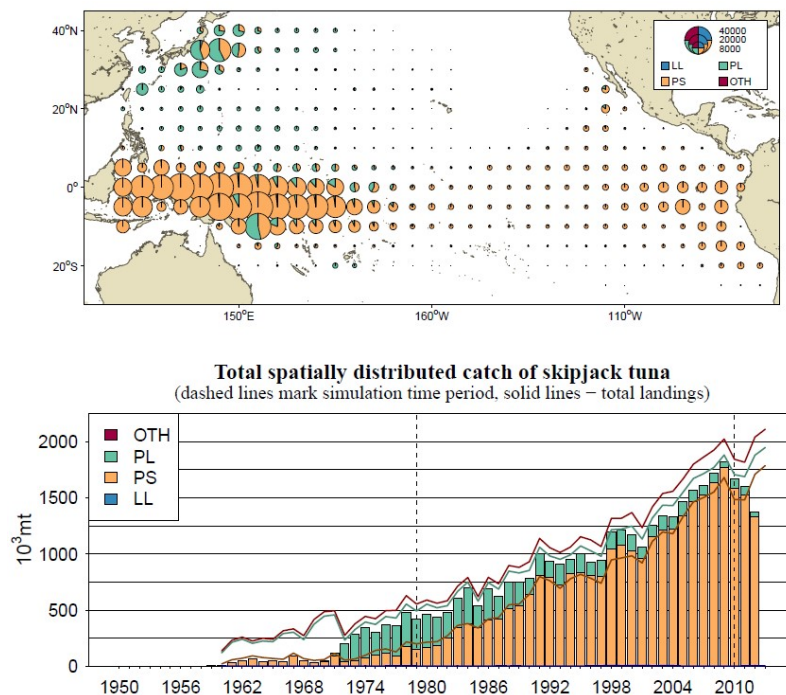

Figure 2: Skipjack catch used in this study. Top panel: total spatially-distributed catch. Bottom panel: Comparison of total annual catches from spatial fishing dataset and from declared port landings (SPC Year Book, 2012).

3.2. Reference optimization (INTERIM)

The new long-term reference solution, hereafter INTERIM, is numerically solved on a 2° regular grid at monthly time step. The age structure of skipjack is discretized between 0 and $age_{max} = 4$ (yr) into monthly cohorts resulting in 37 cohorts. The first three years are split into 36 monthly age classes and the oldest individuals are aggregated into the last single cohort. Age-length and age-weight relationships were derived from the 2014 MULTIFAN-CL estimate (Rice et al., 2014). The species is assumed to be opportunistic spawner with a spawning success proportional to the

spawning habitat index and the larvae stock-recruitment (Beverton and Holt) function computed locally at the cell level.

The initial conditions at the beginning of the simulation (1979) were obtained using the previous reference configuration (see (Lehodey et al, 2014). The catch removal method was used for East-Asian fisheries (Philippines-Indonesia) for which there is no fishing effort available and also for the purse seine fisheries that provide a too noisy signal in the fishing effort. A prior information to constrain the average stock value was added to the likelihood function with the objective to find the minimal stock given the spatial distribution predicted by the model that supports all local catch levels, based on a criterion of less than 20% discrepancy between total observed and predicted catch by fishery. This value was estimated to 8,000,000 mt Pacific wide (120°E – 70°W, 20°S – 45°N). This new reference optimization (Figures 3 and 4) corresponds to the experiment E3 in Senina et al (2016).
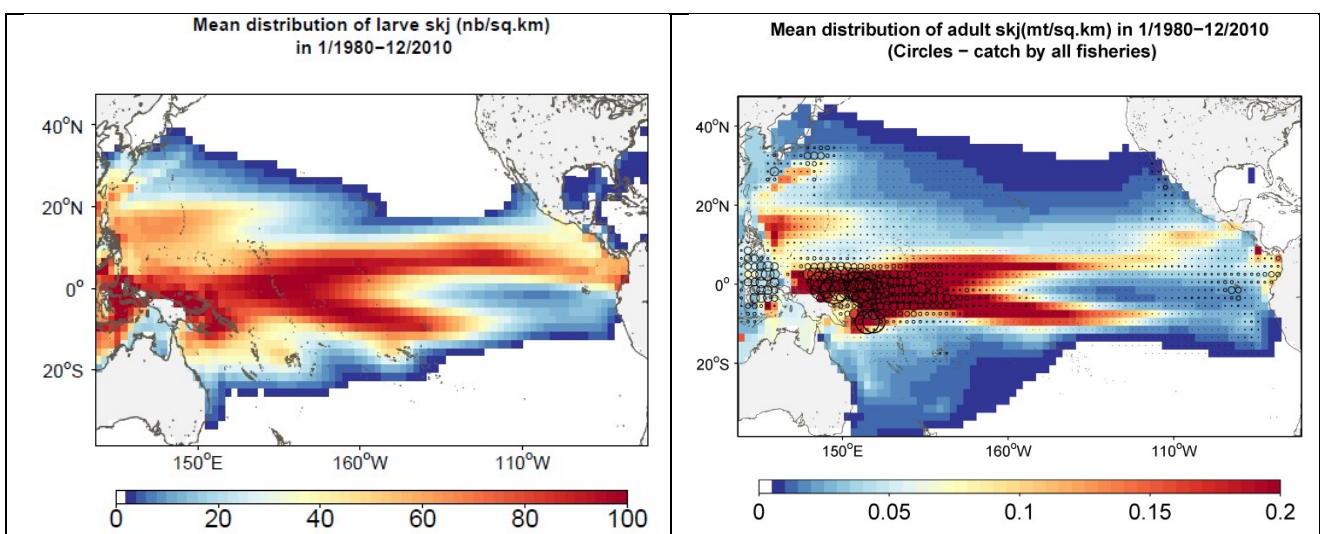

Figure 3: Average spatial distributions of skipjack larvae (left) and adult (right) biomass predicted with selected reference optimization (E3) experiment.
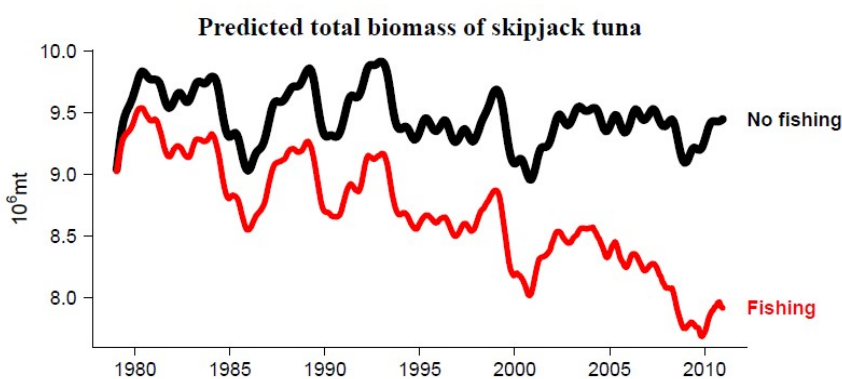

Figure 4: Time series of predicted total skipjack biomass with and without fishing (E3 reference simulation shown by thick lines)

3.3.   Downscaling to high resolution configuration (GLORYS)

The coarse resolution used with the reference simulation INTERIM above allows to solve the large oceanic circulation but not the mesoscale activity in the ocean that has strong influence on the distribution of micronekton (tuna prey) and tuna biomass. Since it is yet difficult to conduct optimization experiments at high resolution due to computational requirements, one alternative solution to investigate the impact of ocean mesoscale activity on skipjack distribution is to

downscale the reference parameterization to the new configuration at higher resolution. Given the sensitivity of SEAPODYM model to the oceanic circulation and the importance of currents for this connectivity study, a careful study of different high resolution ocean reanalyses has been conducted. The analysis focused on the circulation in the warmpool and its connection with the Kuroshio Current.

A downscaling approach has been developed and applied using the selected ocean reanalysis with intermediate steps woth resolution at 1°x month, ¼° x month, and finally ¼° x week. The downscaling uses the MLE framework to re-estimate the habitat and movement parameters using the habitat and density outputs generated with the reference parameterization. Once these parameters were estimated the demographic parameters and age structure, which depend on the temporal resolution, were revised. The initial condition that is the model state vector (densities at age) were redistributed to 163 weekly cohorts. Finally high resolution model outputs were validated using high resolution fishing data (purse seine fishing data provided by SPC).

3.4.   Simulations for the connectivity study

Outputs of both coarse and high resolution simulations were used and compared together and with recent studies using the definition of regions proposed by Kiyofuji (2016) (Figure 5).

a series of simulations were run to investigate the connectivity between these regions. Using the simulation without fishing as a reference, new simulations are produced for each region where all recruits or adult cohorts were "killed" in the model in the selected zone. Then by measuring the change with the reference simulation, it is possible to quantify how much this "donor zone" contributes to the other region(s).

Finally, the impact of equatorial purse seine fishery on biomass and other fisheries was tested by running a simulation with purse seine fishing effort (catch) set to zero and the results compared to the reference the simulation including all fishing.
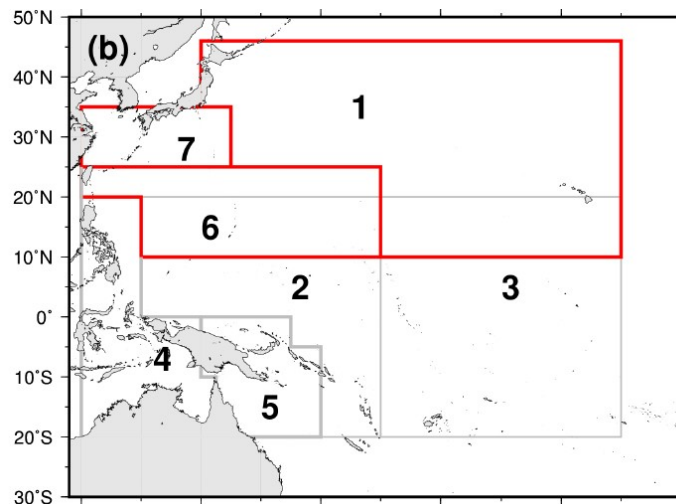

Figure 5: Area definition used by Kiyofuji (2016).

4. Results

4.1.   Oceanography and selection of high resolution ocean reanalysis

The following ocean reanalyses/systems were first carefully analyzed:

- **HYCOM** (2010-2012; Global; 1/12°): Navy Reanalysis at 1/8° (1995-2012), with data assimilation based on Multivariate Optimal Interpolation
- **GLORYS2V4:** Most recent Mercator-Ocean reanalysis (1992-2015) at 1/4° using NEMO ocean circulation model and data assimilation system SAM2 (Bias correction + DA based on SEEK filter)
- **GLORYS2V4_free:** Same as above but without data assimilation
- **PSY3V4R1** (2007-present ; 1/4°)**:** same as GLORYS2V4 with only bias correction:
- **ECCO:** MIT Ocean General Circulation Model (MITgcm) at 1°x1° + data assimilation using Dual Kalman filter and adjoint assimilation schemes.
- **ORAS5**: ECMWF reanalysis at 1/4° (1975 to present) with NEMO and 3DVAR data assimilation scheme.
- **GOOP**: CLS geostrophic velocity from thermal wind equation (ARMOR3D) using satellite data (altimetry and SST).

Zonal currents in the Western Pacific Warm Pool from these different model products (climatology 2010-2012) are shown below and compared to observation climatology AOML (annual) and drifters data for the same period 2010-2012. The South Equatorial Current (SEC), North Equatorial Current (NEC) and North Equatorial Counter Current (NECC) are predominant features of the ocean circulation in the warm pool. The SEC and the NEC are of primary importance to understand what is going on further north via the Kurushio current (it could explain partly the connection between the equator and Kurushio). The westward flowing NEC runs into the Philippine coast and bifurcates between 12° and 15°N into the northward Kurushio and the southward Mindanao Current. The transport of the Kuroshio vary with the transport of the NEC and the location of its bifurcation point (Hsin et al., 2008 ; Qiu and Lukas, 1996; Qu et al., 1998; Kim et al., 2004). Based on two consecutive research cruises in 2011 n 2012, Gordon et al. (2014) observed a shift in latitude of the NEC bifurcation with more southern position in 2012 that could result in a stronger connectivity between equatorial circulation and northwards transport (Figure 6). The NEC and the Mindanao currents seem to be key points to have a good representation of the connection between lower latitudes circulation and the Kuroshio current.
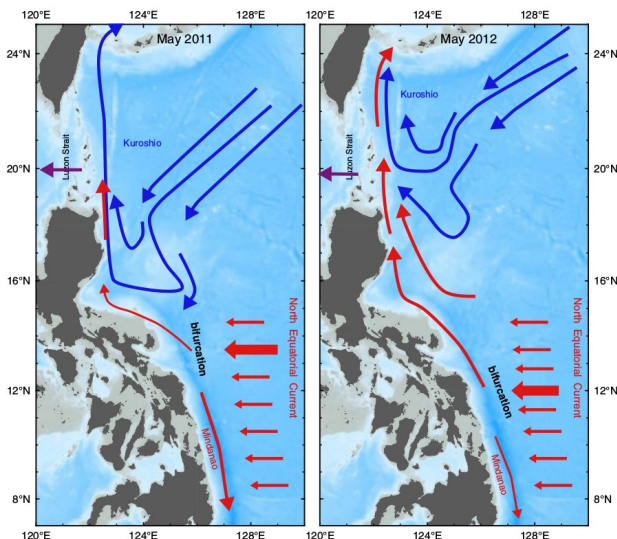

Figure 6: Schematic of observed change in ocean circulation along the Philippine coast and Kuroshio path based on two consecutive research cruises in May/June 2011 and April /May 2012 (Gordon et al 2014).

A seasonal maximum in Kuroshio transport usually occurs in the fall (September–October) when the bifurcation point of the North Equatorial Current is northernmost (Qiu and Lukas, 1996; Qu et al., 1998). Because of the connection between the Kuroshio and the equatorial current system, it is not surprising that variations of the Kuroshio at timescales of 3–7 years (ENSO) could be traced to those in the North Equatorial Current (Qiu and Lukas, 1996). The Kurushio is also an important source of tropical waters for the China Sea via the Luzon strait (Tranchant et al., 2016).

The New Guinea Counter Current (NGCC) flowing along the eastern coast of New Guinea is another key feature of the regional circulation, flowing northwestward. It intensifies during the boreal summer, then weakens or even reverses direction to southeastward during the boreal winter. In sub-surface, the New Guinea Coastal Under Current (NGCUC) flows northwestward all year-round and intensifies during the boreal summer and growing phases of El Niño events. This circulation is associated with a coastal upwelling that seems critical to simulate for a good understanding of the dynamics of the region and its high productivity for tuna fisheries. Finally, the numerous islands and straits of the Southwest Pacific generate boundary currents and jets that eventually redistribute water to the equator and high latitudes (see Ganachaud et al., 2014).

ECCO has a too coarse resolution to properly simulate North Equatorial Counter Current (NECC) and North Guinean Counter Current (NGCC), but it simulates quite well the South Equatorial Current (SEC: westward) which starts decreasing from 170°W, as well as ORAS5 and G2V4 free reanalyses (Figure 7). The SEC is predicted too intense in GLORYS2v4, PSY3v4R1 and HYCOM. The NECC is also too strong apparently with HYCOM. All simulations are affected by ENSO, with la Nina (ENSO-) in 2010 strengthening the SEC whereas the SEC has a lower extent in 2012 during moderate El Nino (ENSO+). NGCC and NGCUC are very strong in ORAS5 and not present (or very weak) in HYCOM which is surprising since the horizontal resolution is higher. They are also not present in AOML due to the too coarse resolution of data (1°x1°). GLORYS2v4-free and ORAS5 seem to provide the best compromise for the equatorial circulation, though ORAS5 has a weaker NECC.

In higher latitudes, the products using data assimilation perform better. This is particularly clear with the position of the Kuroshio extension (Figure 8) that is not well represented in GLORYS2V4-free.

Given the importance of equatorial circulation for a good representation of tuna stock dynamics in the warm pool, the reanalysis GLORYS2V4-free was selected despite its lower accuracy in the representation of the Kuroshio extension which is less critical for this connectivity study. However, it is available only for the period 2006-2015. The impact of equatorial circulation simulated by different models on skipjack dynamics is highlighted on figure 9.
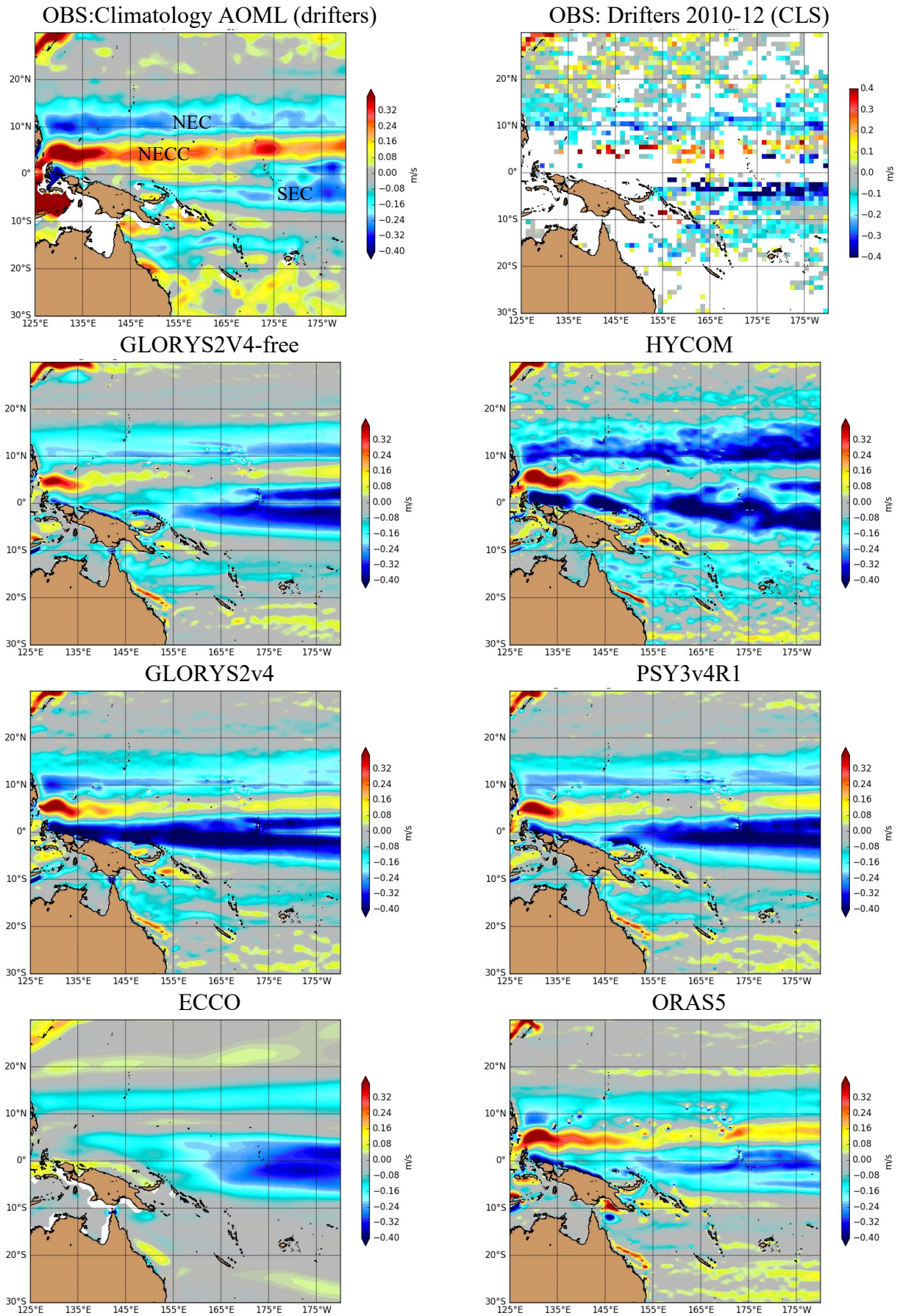
Figure 7: Zonal surface currents from observations and different reanalyses/operational models
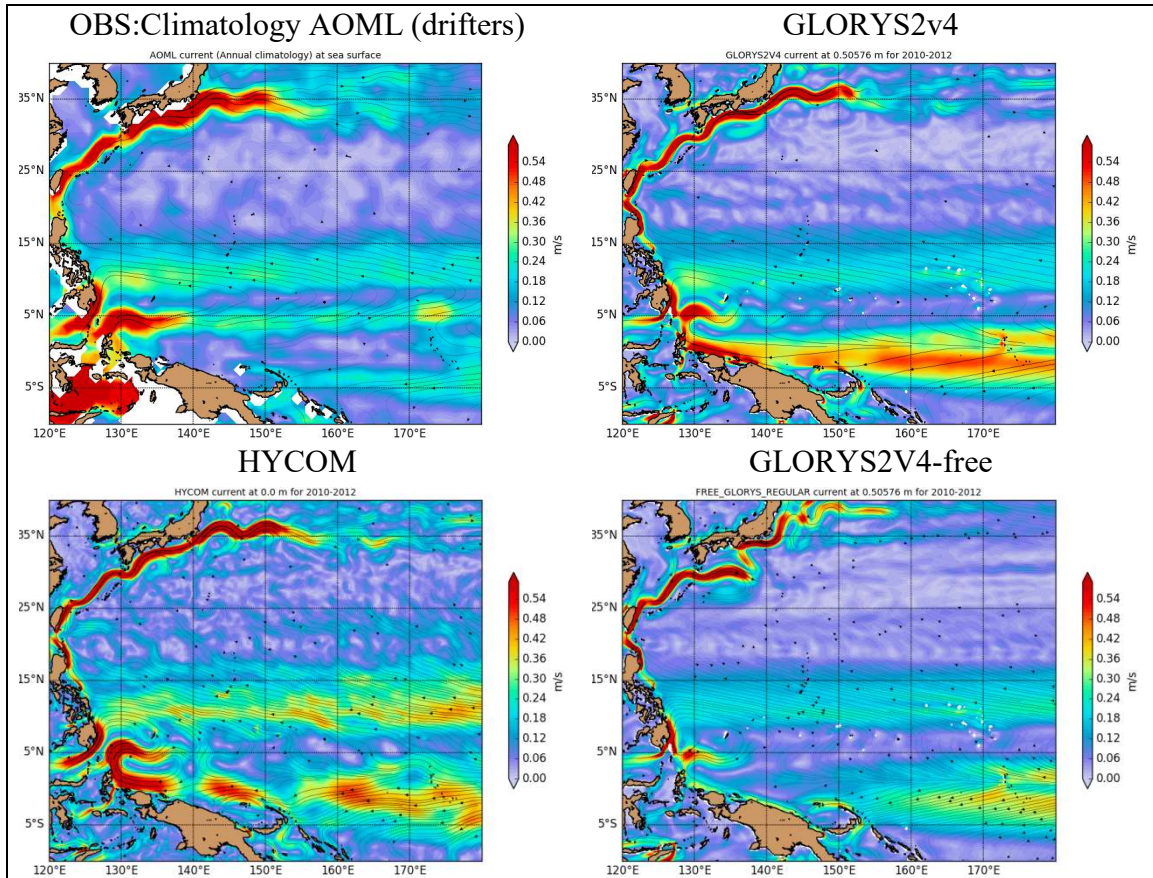
Figure 8: Surface current for different simulations (2010-2012) compared to AOML climatology
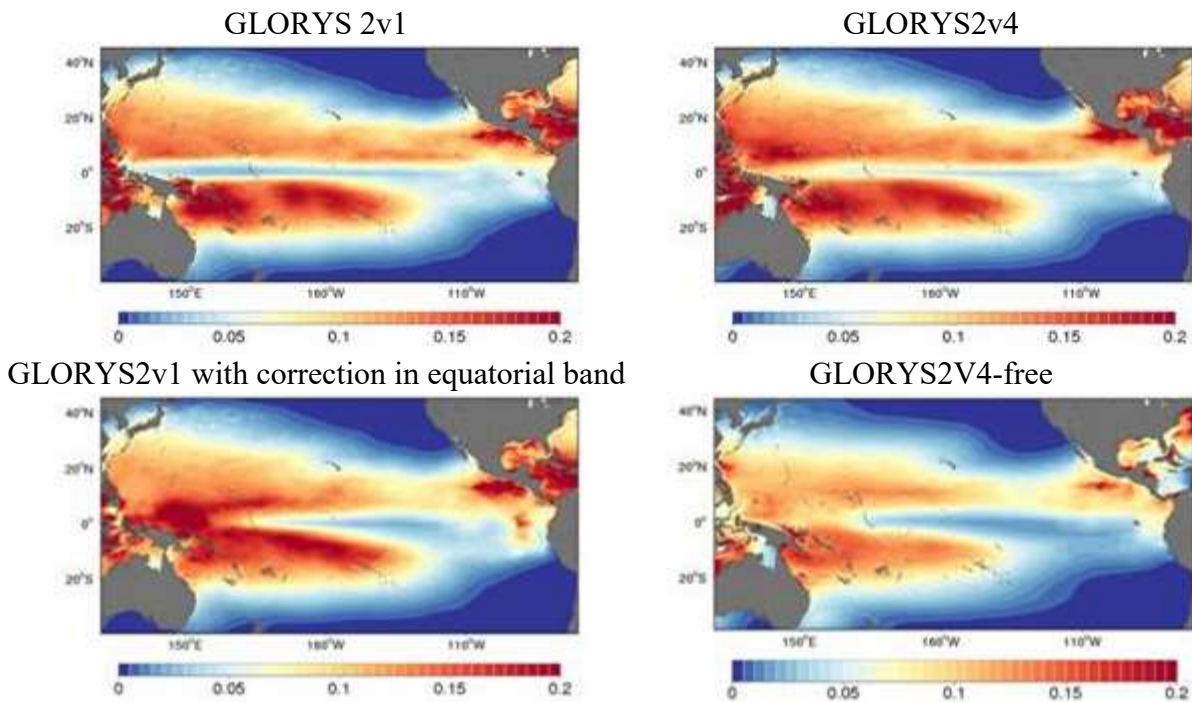

Figure 9: Average annual density of skipjack tuna predicted with 4 different physical forcings to test the sensitivity of results to equatorial circulation.

4.2. Reference INTERIM-2° simulation

Estimated model parameters driving population dynamics are listed in Table 1. The optimal spawning temperature was estimated to 28.5 °C (std. er. 1.48°C). The thermal habitat of the species function ranges between 28.5 and 26°C (Appendix ; Figure A2). These estimates are in good agreement with current knowledge. The species is opportunistically spawning in waters between 26°C and 30°C (Schaefer, 2001), and has an overall distribution identified from all historical occurrences between sea surface temperature of 17°C and 30°C (Sund et al., 1981). The values of the oxygen function parameters were well estimated and indicate a low tolerance of the species to poorly oxygenated waters (threshold value of 3.6 mL/L; Table 1).

This parameterization leads to seasonal favorable "hot spots" for spawning in the EPO (April to June with maximum in May), central Pacific (May-August) and in the north-west of East China Sea (spawning habitat is close its maximum value in August-October). Some seasonality of the spawning index is also predicted in Bismarck Sea, where the larvae densities are high from May to November, while very little spawning occurs between December and February.

The current temperature estimate implies the accessibility of skipjack only to forage available in the epipelagic layer. This is also seen from the estimates of MTL groups contributions to the habitat (appendix: Table 1), which are estimated non-zero only for resident epipelagic and highly migrant bathypelagic forage, that migrate to surface layer at night.

The larvae stock-recruitment functional relationship (between the spawning biomass and the amount of larvae recruited in the first month cohort) has been estimated (Table 1 ; Figure A2). It shows increasing sensitivity for density below 10 adult indivuals per square kilometer. Given that most adult skipjack average density is estimated to be less than 0.2 t/km^2 (Figure 3), this suggests a relatively strong sensitivity of larvae recruitment to the spawning biomass.

Once a maximum -- rather theoretical -- value of natural mortality has been fixed, the other parameters defining the functional form of average natural mortality-at-age can be estimated. It gives mean natural mortality rates within the range 0.15 - 0.25 mo^{-1}, slightly higher than those estimated with Multifan-CL between 0.09 - 0.22 mo^{-1} (Appendix: Figure A2).

The predicted skipack density distributes mostly in the warmpool in the tropical area where is the main fishing ground (Figure 3). Two smaller patches of concentration appear in the western Pacific, in the region of the bifurcation point of the North Equatorial Current (cf. Figure 6) and in the Kuroshio Current area east of Taiwan Is.

While the total stock estimates in WCPO are close between SEAPODYM and Multifan-CL (Rice et al., 2014), i.e. 3.4Mt of adult and about 4Mt of total biomass in 2010, a striking feature is the discrepancy in the north Pacific region covering the north west Pacific, where MULTIFAN-CL estimate of skipjack biomass is much higher and variable (Appendix: Figure A3). On the other hand SEAPODYM predicts higher biomass in the two core tropical regions (2 and 3) known to be the main fishing grounds for skipjack. Predicted recruits and adult biomasss in revised definition of regions shown in figure 5 are provided in appendix (Figures A4 and A5).

Despite much lower predicted biomass in region 1, SEAPODYM can predict rather well the catch of the subtropical Japanese pole-and line north of 20° N based on the observed effort (Figures 10 and 11). Note that the fit to catch data of all other fisheries is detailed in Senina et al (2016).

The fishing impact (Appendix, Figure A6) is calculated as $(B_{F0}-B)/B_{F0}$ and is estimated at basin scale to have increased over time to reach 20-25% of reduction by the end of 2010 in average (Senina et al. 2016). However, it is approaching 40 % in regions where the fishing exploitation is the most intense (regions 2 and 5). The fishing impact is predicted to remain quite low (10%) in the region 1 (Figure A6). This is obviously based on catch data declaration and does not take into account possible unreported or illegal fishing.
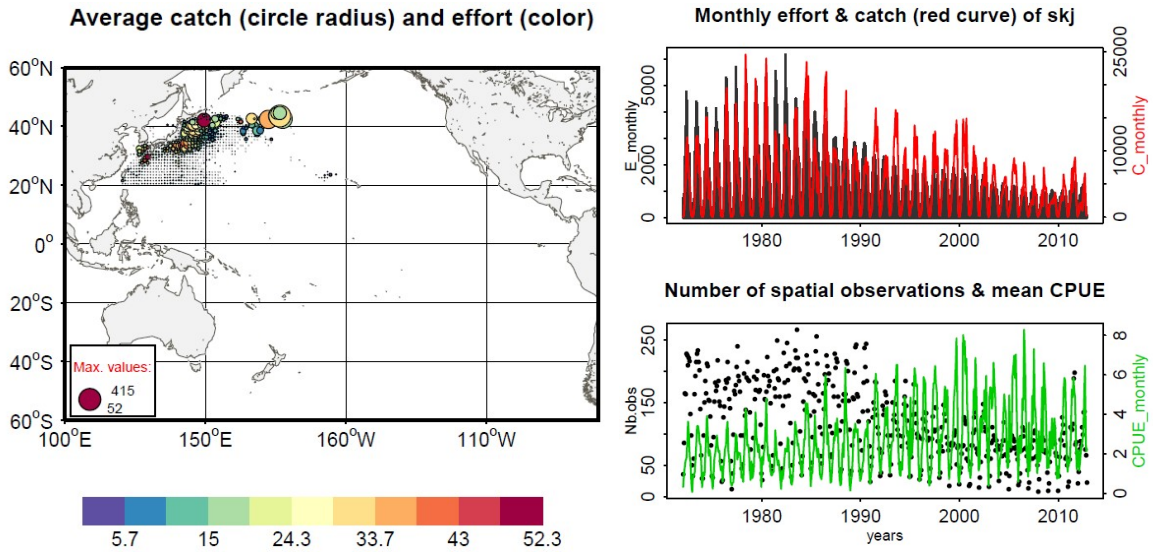
Figure 10. Spatial distribution of subtropical Japanese pole and line fishery data and change over time of catch effort and CPUE.
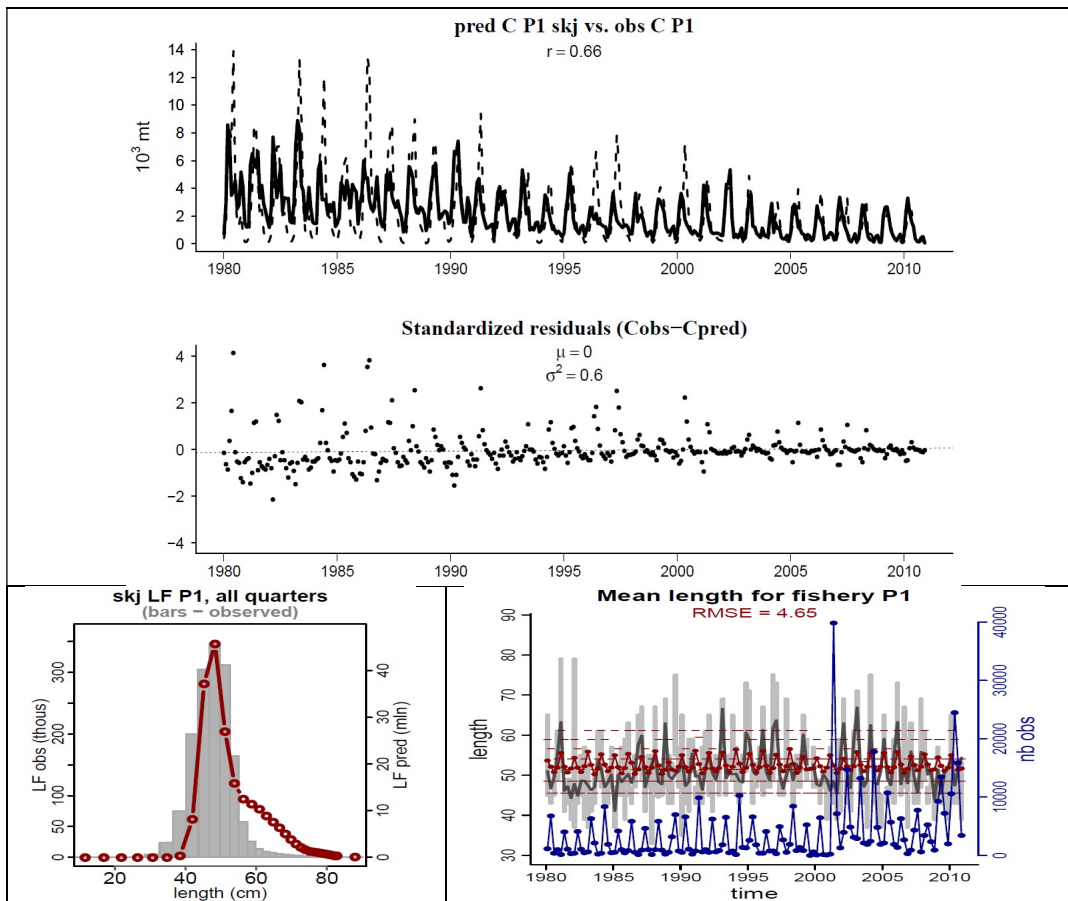

Figure 11. Subtropical Japanese pole-and line fishery. Top: Observed (dotted line) and predicted (continuous line) catch with the reference INTERIM and associated residuals. Bottom: Observed and predicted length frequency of catch with all data distribution (left) and mean length and 95 percentile by quarter over the full time series (right).

4.3. Downscaling to high resolution

Changes in parameter estimates due to the downscaling approach are shown in Table 1. They are minor concerning the thermal habitat for spawning, while for the feeding adult habitat the revised optimal temperature of the oldest cohort increased by ~1.5 °C with GLORYS ($T_K = 27.56°C$). However this is mainly due to a simulated « warmer » (but more realistic) ocean with GLORYS than with INTERIM, especially outside the tropical region. For movement parameters, a striking change is the sensitivity of diffusion coefficient to habitat (c changing from ~1 to ~0) meaning a much rapid decrease of diffusion with increasing habitat values.

Table 1: Parameter estimates achieved with the reference optimization experiment (INTERIM) and subsequent changes due to downscaling approach (* optimization; ** rescaling).

Parameter		INTERIM 2x30d*	INTERIM 1x30d*	GLORYS 1x30d*	GLORYS 025x30d*	GLORYS 025x7d**
σ_0	Std dev of Gaussian for SST for spawning function	1.48		1.45		
T^*_0	Optimal SST for larvae	[28.5		28.71		
T_0	1st young cohort	31.1]		30.17		
α_P	prey encounter rate in Holling (type III) function	0.078		0.0173		9e-04
α_F	Log-normal mean parameter predator-dependent function	2.48		5]		
β_F	Log-normal shape parameter in predator-dependent function	2.5		3.26		
R	Reproduction rate in B&H function	0.2041				0.043
b	Slope parameter in B&H function, nb/km^2	0.4858				
σ_a	Std dev of Gaussian for Temperature for oldest cohort	[1		1.48	[1.35	
T_K	optimal temperature range for the oldest adult cohort	25.93		27.56		
b_T	Scaling exponent in relationship between optimal temperature at age and body length	1.994		1.84		
γ	Slope coefficient in oxygen function	1e-6				
O_{cr}	Threshold value of dissolved oxygen, ml/l	3.642				
eF_1	contribution of epipelagic forage to the habitat	4]	1.54	2.61		
eF_2	contribution of upper mesopelagic forage to the habitat	0.05		[0		
eF_3	contribution of migrant upper mesopelagic forage to the habitat	[0		0.0154*		
eF_4	contribution of bathypelagic forage	[0				
eF_5	Contribution of migrant bathypelagic forage	[0				
eF_6	contribution of highly migrant lower mesopelagic forage to the habitat	1.8914	1.9333	1.7184		
σ	Coefficient of diffusion	0.177			0.1879	
c	coefficient of diffusion variability with habitat index	0.9414	0.6626		[0.000	
V_m	maximal sustainable speed	0.7766	2.2258			
a_V	Slope coefficient in allometric function for maximal speed	0.8349				
m_p	predation mortality rate age age 0	0.25				0.0598
β_P	slope coefficient in predation mortality	[0.0504				0.0118
m_s	senescence mortality rate at age 0	0.0099				8e-04
ε	Variability of mortality rate with habitat index	[0				

The approach has been validated by comparison with biomass predicted from the reference coarse resolution INTERIM (Figures 12 and 13). Then, the fit to fishing data was evaluated with usual metrics (appendix: Figure A7) and with high resolution purse seine fishing data provided by SPC (appendix: Figure A8). High resolution Japanese domestic catch data were not used due to the bias

identified in the position of the Kuroshio extension. The match between high catch and high density of (exploitable) skipjack in the equatorial purse seine fishing ground is particularly good (appendix: Figure A8). This is notably also the case in the Solomon Is. and Papua New Guinea region (including Bismark Sea), where previous tentatives with a first version of GLORYS reanalysis were not conclusive and obliged to apply a correction on the mean state of the circulation in the equatorial band 10°N-10°S (Figure 9). This is therefore a major progress and encouraging results for further studies based on this model configuration.
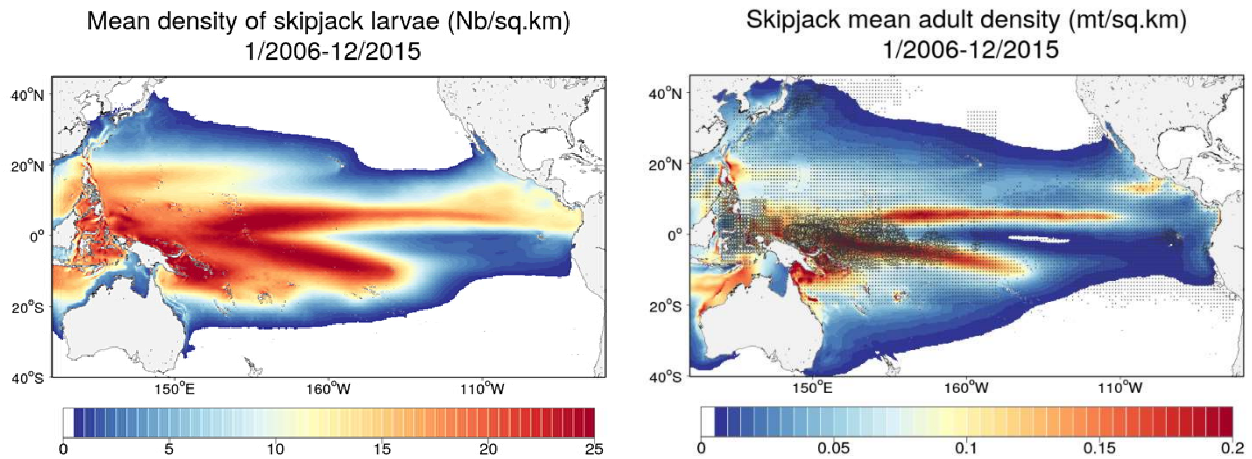

Figure 12: Average spatial distributions of skipjack larvae (left) and adult (right) biomass predicted over 2006-2015 with the high resolution GLORYS2v4-free simulation with total catch for the period shown with circles proportional to catch.
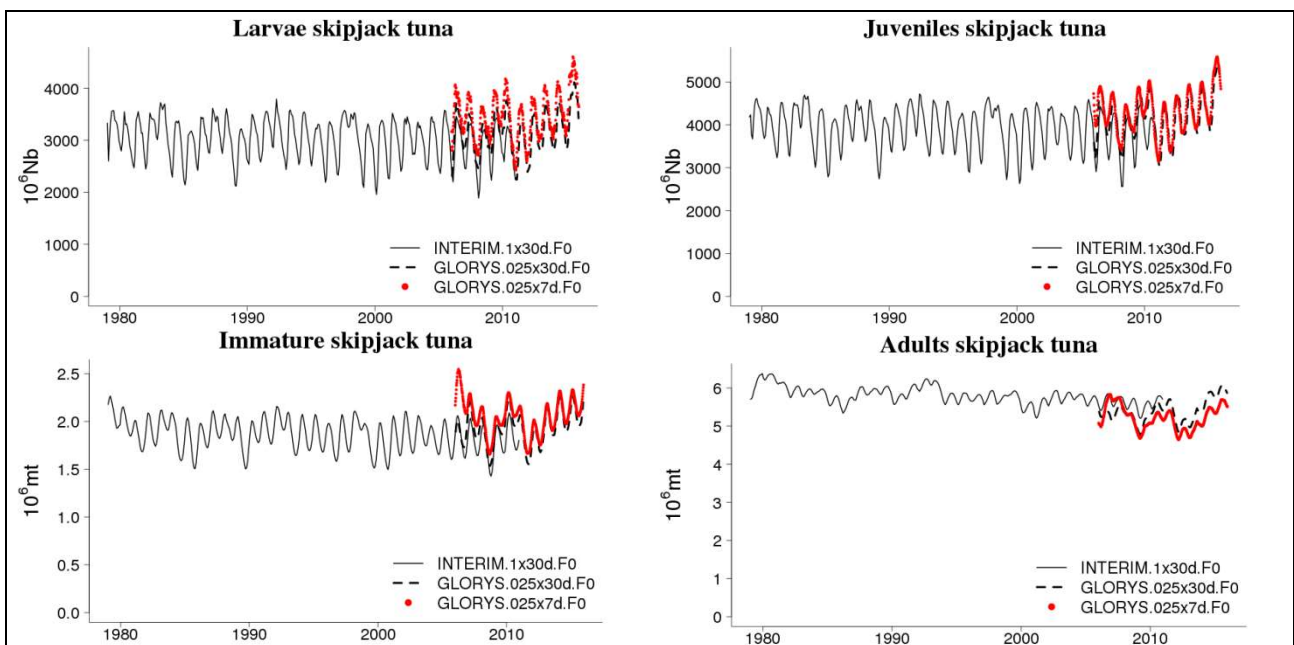

Figure 13: Superimposition of biomass by life stage predicted with the INTERIM reference simulation (1980-2010) and the GLORYS2v4-free high resolution simulation (2006-2015).

The fit of the high resolution simulation GLORYS to the Japanese subtropical pole and line catch data is high (r =0.73) and does not predict a change in the size frequency of catch as suggested by the slightly lower mean size sampled between 2008 and 2010 (Figure 14). Peaks of observed catch are also not well predicted. But it may be not too surprising given the bias known on the predicted circulation in that region.

Predicted biomass of the high resolution 2006-2015 GLORYS simulation in region 1 and 7 have been extracted and overimposed to the historical time series estimated with the INTERIM simulation (Figure 15). The first 3 months, 12 months and 24 months have been removed respectively for larvae, immature and adult fish as they are strongly linked to the initial conditions provided to GLORYS simulation. There are interesting trends suggested by this simulation in the recent years. In region 1, after a tendency to decrease over 2006-2012, the larvae recruitment shows an opposite increasing trend in the recent years. This signal is delayed in immature cohort and then adult cohorts. The immature biomass shows an increase in the last year (2015) of the simulation while it is not yet appearing in the adult stock but could be expected in 2016-17.

In region 7, density of recruited larvae is predicted to be lower with GLORYS than with INTERIM. A slightly decreasing trend also occurs in predicted recruited larvae. Biomass of immature and adult cohorts follows the same trends with delayed effect as those observed in region1.
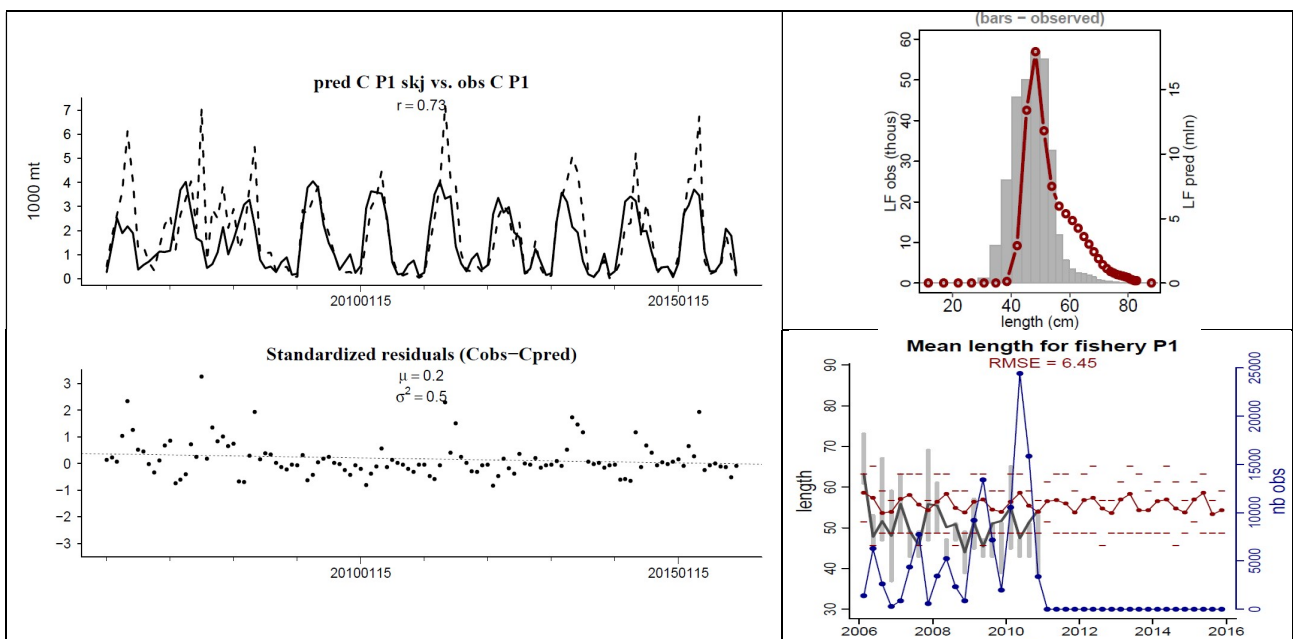

Figure 14: Region 1 and subtropical Japanese pole-and line fishery. Top: Observed (dotted line) and predicted (continuous line) catch with the downscaled simulation GLORYS2V4-free and associated residuals. Bottom: Observed and predicted length frequency of catch with all data distribution (left) and mean length and 95 percentile by quarter over the full time series (right).
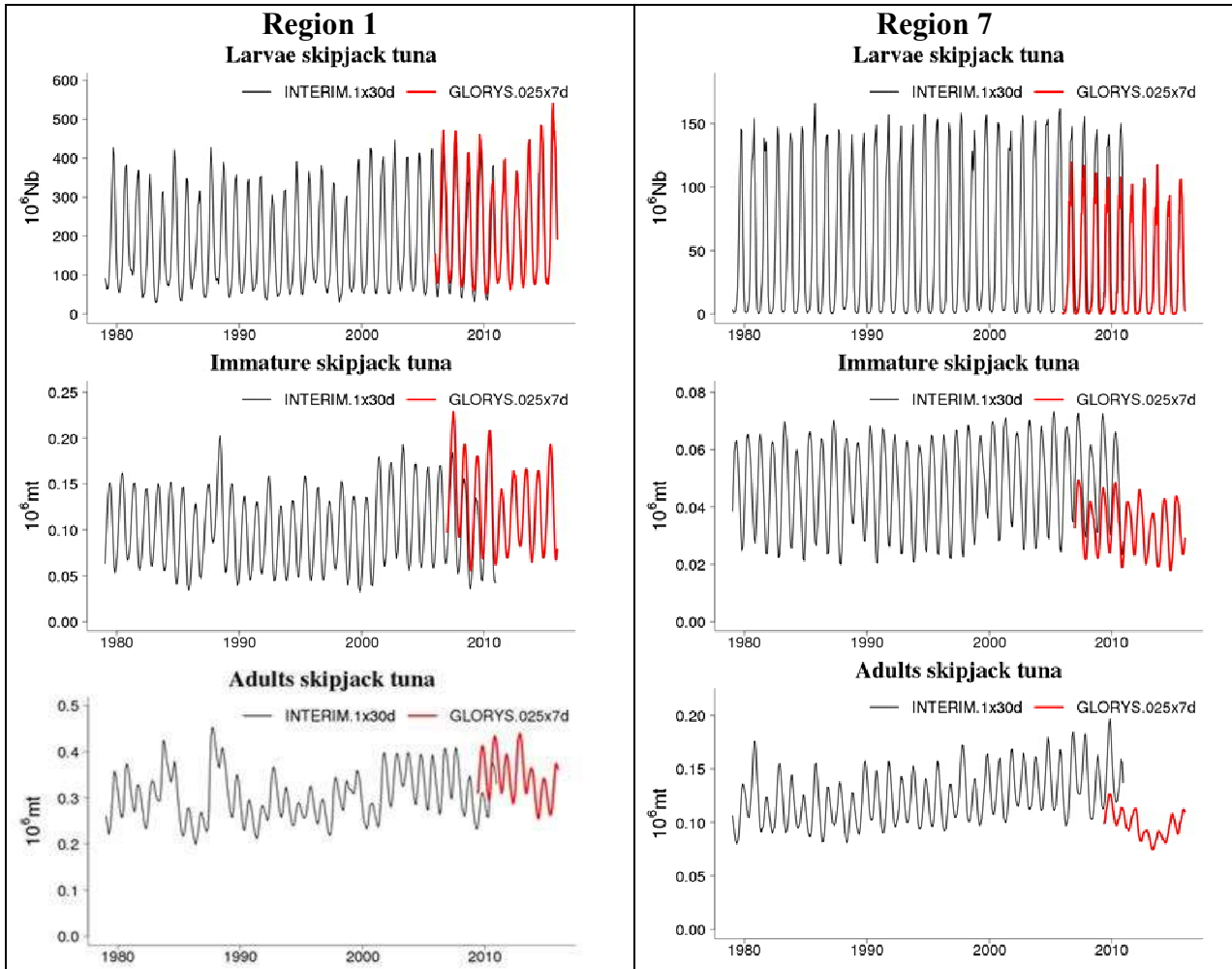
Figure 15. Change in biomass in regions 1 and 7 for larvae immature and adult skipjack from the INTERIM simulation, continued with the GLORYS high resolution outputs.

4.4. ENSO variability

Extended displacement of skipjack tuna in relation with El Niño Southern Oscillation (ENSO) events have been demonstrated from fishing and tagging data in the equatorial Pacific (Lehodey et al. 1997). The impact of the recent El Niño event that occured in 2015 (and early 2016) is well visible on Figure 16 (and Figure A8 as well). It is useful to note that though this event was intense it did not reach the Eastern Pacific Ocean, and belongs to the category of central El Niño event also called Modoki (Appendix Figure A9).

Both the coarse (INTERIM) and high resolution (GLORYS) simulations predict the large east-west displacement of skipjack in the equatorial region associated to ENSO and in correlation with the observed changes in purse seine fishing grounds (Figure A10). In addition to redistribution of fish, these simulations confirm that ENSO also impacts the recruitment of Pacific skipjack with larger spawning habitat and recruits during El Nino phases. This is particularly clear in the outputs of the GLORYS high resolution simulation (appendix Figure A10), with high correlation between the Southern Oscillation Index (SOI) and the density distribution of juvenile skipjacks, and the subsequent delayed correlation with adult biomass (Figure A10). The increasing larvae recruitment observed in region 1 above (Figure 15) is therefore likely associated to the favorable spawning conditions occuring during the El Niño event that started in end of 2014 and last until early 2016.
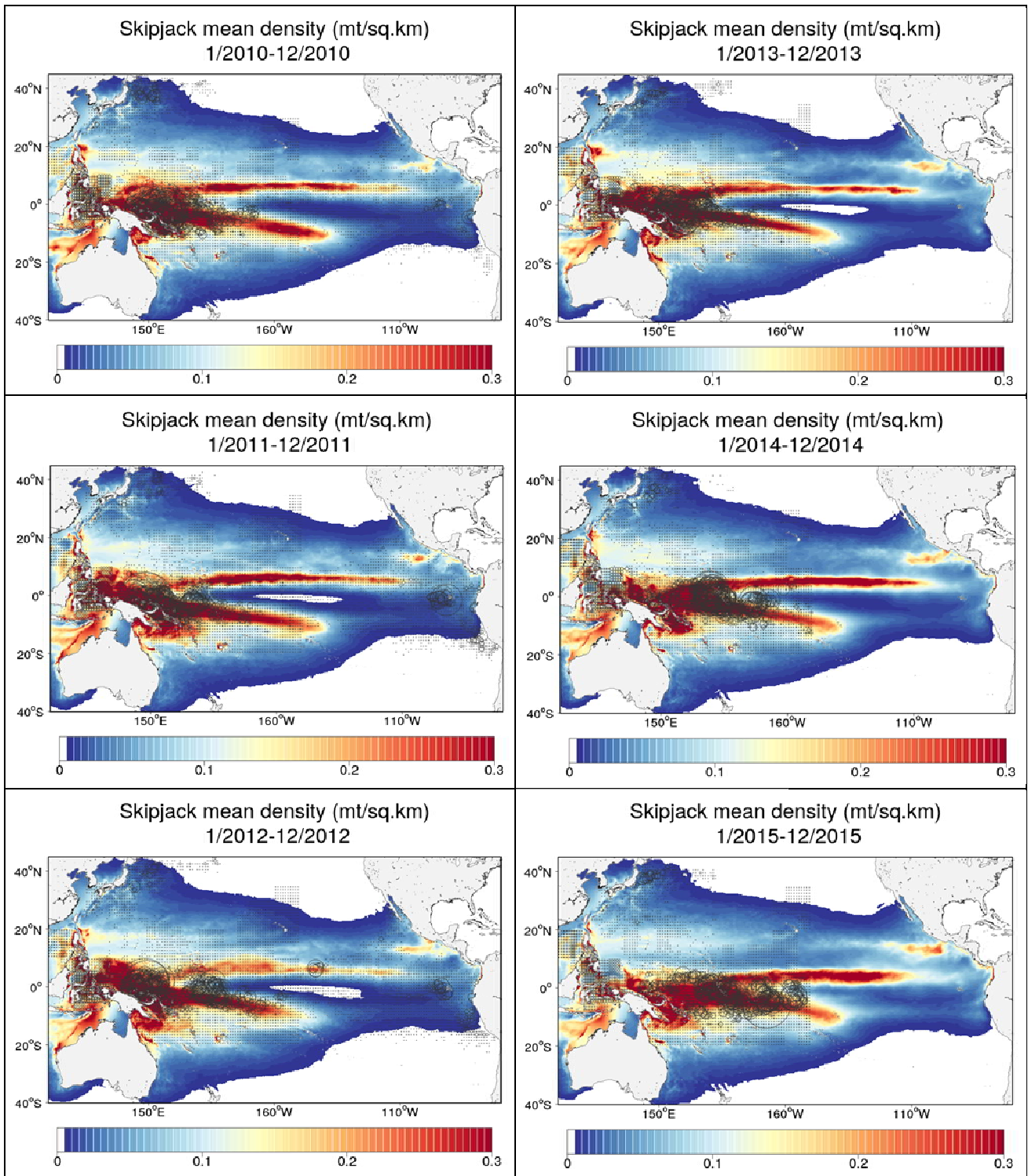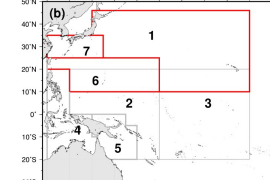
Figure 16: Annual mean distribution 2010-15 of total skipjack from GLORYS 0.25°/week simulation with total catch overimposed as circles prorportional to catch. Note the change due to El Niño in 2015.

4.5. Connectivity simulations

For each region proposed by Kiyofuji (2016) (Figure 5), two simulations are produced with both model configurations (INTERIM and GLORYS2v4-free) with all recruits or adult cohorts "killed" in the model in the selected region. There are relatively slight differences in the distributions of adult biomass predicted by region between the two simulations (Table 2). The largest discrepancies occur in equatorial regions 3 and 4 but are limited to <~5% of the total biomass.

Then by difference with the reference simulation we can quantify how much the "donor zone", where the recruits or adults have been killed, contributes to the other region(s). The results are presented in Table 3 and 4 for recruits and adults respectively.

Table 2: Percentage of adult (spawning) skipjack biomass by region

	Region1	Region2	Region3	Region4	Region5	Region6	Region7
INTERIM 2°	5.4	27.2	32.3	9.1	14.3	9.4	2.3
GLORYS2V4-Free 0.25°	7.7	25.4	26.9	13.7	13.9	10.0	2.4

The change in adult biomass by region is computed over the last 5 years (2006-2010 for INTERIM and 2011- 2015 for GLORYS) of the simulations and in absence of fishing. Therefore, coarse and high resolution simulations are covering different time periods and are not strictly comparable. The percentage change is computed relatively to the biomass of reference simulations.

When setting recruitment to zero in the different regions, the largest difference between these simulations occurs for region 7 where the adult biomass decreases by 47.3 or 18.1 % respectively for the INTERIM and GLORYS simulations suggesting a strong sensitivty to mesoscale circulation in this region. Recruitment in this region 7 is predicted to have only moderate connectivity with adult biomass in adjacent regions 1 and 6 and almost no impact in other regions. On the other hand, recruitment in region 6 is strongly supporting adult biomass in region 7 in addition to its own biomass and, to a lower level, the adjacent regions 4 and 1. Region 4 is also well connected to region 7 likely through NEC and Kuroshio currents system.

Recruitment in the tropical region 3 covering part of the main purse seine fishing ground support its own adult biomass to a high level (decrease >50 % in absence of recruitment in this region) and also the adjacent regions 2, 5 and 1. Recruitment in region 2, the other main tropical purse seine fishing ground would also strongly support adjacent region 5 and 4 and to a lower level region 6.

Adult biomass in region 1 would be supported by recruitment in its own area (~30-35%), then the region 3 (~24- 38%), region 6 (~10-25%), region 7 (~5-13%) and 2 (~5-10%).

By using the same approach but setting adult cohorts rather than recruits to zero in each region, the idea is to investigate a more direct connectivity including movements of adult fish from one region to an other. In that case all regions are shown to largely support their own adult biomass (Table 3) with consecutive decreases > 80%. However, the simulations also suggest connectivity that are resulting of exchanges between regions rather than direct transfert of biomass. Therefore, when adult biomass is set to zero in central region 3, it strongly decreases the adult biomass in regions 1, 2 and 5. Adult biomass in region 1 is connected strongly to regions 3 and 6 (as for recruits). More generally these simulations confirm the connectivity results described for recruits. They are

synthesized in a schematic diagram (Figure 17) with three levels of intensity in connections. It highlights the strong connectivity in the equatorial band and also along the current system with the NEC and the Kuroshio on west side and between central region 3 and north Pacific region 1 on the other side. The relatively weak link between region 7 and 1 is likely due to the very large area of region 1. It could be useful in a revision of this analysis to divide region 1 in two sub-regions, e.g. east and west of 170°E.

Table 3: Change (% decrease) in adult biomass due to the absence of recruits in the selected region.

Recruits set to zero in region:	region1	region2	region3	region4	region5	region6	region7
reg1_2°	30.9	5.0	5.4	2.4	1.5	16.2	6.6
reg1_0.25°	35.4	2.7	2.4	0.9	0.2	18.5	3.0
reg2_2°	9.5	39.3	14.8	27.0	44.6	22.0	10.2
reg2_0.25°	5.5	37.9	11.8	22.2	35.2	14.9	2.9
reg3_2°	37.6	48.6	68.9	6.0	39.5	19.1	4.2
reg3_0.25°	23.8	33.9	49.9	5.5	29.1	12.2	0.5
reg4_2°	5.0	6.9	0.3	42.3	6.9	12.2	27.9
reg4_0.25°	2.4	7.8	0.2	42.2	3.5	6.2	28.8
reg5_2°	1.7	18.0	2.8	12.7	35.6	5.0	1.4
reg5_0.25°	0.2	15.6	1.3	11.4	36.8	2.4	0.2
reg6_2°	24.9	11.3	0.9	30.3	5.7	52.8	68.1
reg6_0.25°	10.2	4.1	0.1	16.5	0.7	39.0	45.4
reg7_2°	13.4	1.3	0.1	3.6	0.4	15.6	47.3
reg7_0.25°	5.9	0.0	0.0	0.3	0.0	3.0	18.1

Table 4: Change (% decrease) in adult biomass due to the absence of adult fish in the selected region.

| Adults set to zero in region:	region1	region2	region3	region4	region5	region6	region7
reg1_2°	86.0	5.9	12.1	2.5	1.5	24.8	20.1
reg1_0.25°	98.2	3.7	9.3	1.2	0.5	30.4	14.2
reg2_2°	14.8	90.9	21.4	38.9	68.9	42.0	13.6
Reg2_0.25°	11.5	98.8	22.6	36.6	64.6	35.5	6.6
reg3_2°	44.0	51.2	97.6	5.1	36.5	18.6	3.7
reg3_0.25°	44.4	48.6	99.6	9.2	42.0	18.7	1.3
reg4_2°	4.5	17.1	0.4	88.8	15.7	26.2	29.9
reg4_0.25°	3.7	20.3	0.2	98.5	11.3	16.4	43.9
reg5_2°	3.3	40.2	3.8	20.8	90.2	10.5	2.7
reg5_0.25°	0.4	37.8	1.7	18.1	98.4	5.1	0.6
reg6_2°	36.4	17.9	2.3	31.2	6.0	90.6	81.4
reg6_0.25°	24.0	14.3	1.1	21.4	1.5	98.4	80.1
reg7_2°	16.3	1.6	0.1	4.4	0.4	22.2	84.5
reg7_0.25°	10.5	0.1	0.0	0.7	0.0	8.6	97.6
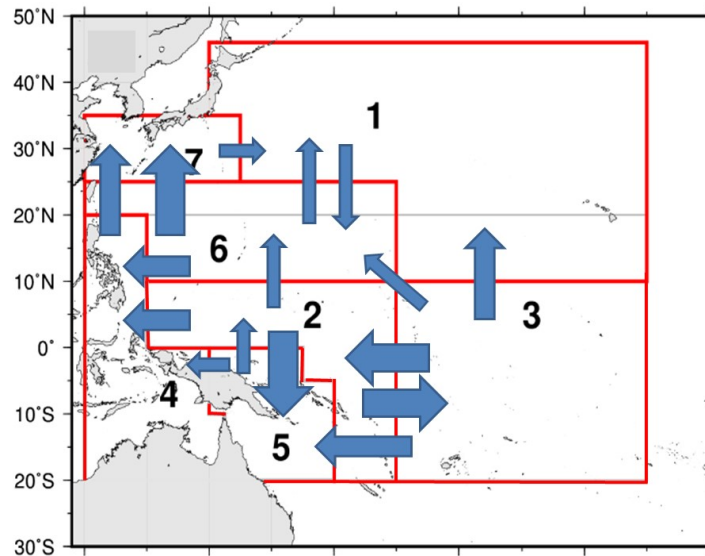
Figure 17: Schematic representation of intensity of connections between regions based on connectivity simulations described in Tables 2 and 3. Links are represented by three categories of arrows for intense, moderate and weak intensity. For clarity, very low connectivity links are not shown.

4.6. Impact of purse seine fishing

A last experiment compares the reference simulation with a simulation without the fishing mortality associated to the equatorial purse seine fisheries (S5 S6 S7 in Table A1). The increase (%) in adult biomass of region 1 and 7 are shown on Figure 18. The increase appears very limited (< 6%) in both. The maximum impact is predicted to occur in the main purse fishing ground with biomass increase above 50% and even >100% locally (Figure 18). Similar results are obtained for the change in catches in the simulation without purse seine fisheries (Figure 18). The total catch in the region 1 (north of 20°N to avoid including the tropical purse-seine catches) increases up to 5% (2010) if the catches by fisheries S5, S6 and S7 are set to zero. For the region 7 the effect of tropical fisheries is much more moderate, exceeding slightly 1%.
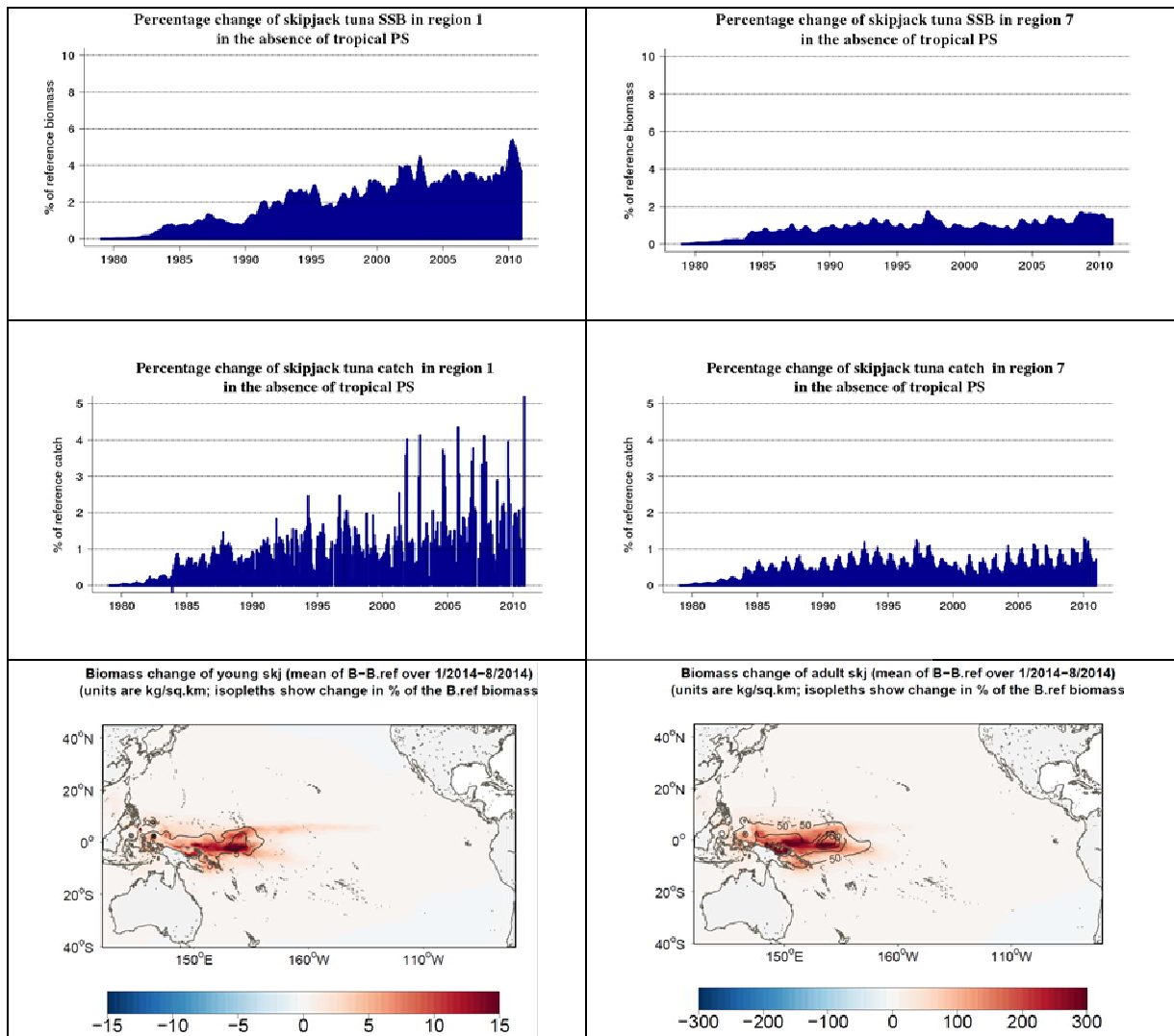
Figure 18: Fishing impact in regions 1 and 7 and its spatial distribution estimated for the last year (2015)

5. Conclusion

Through a careful sensitivity analysis of the SEAPODYM model to oceanic currents provided by various existing up-to date ocean reanalyses, it was possible to select the best forcing and to identify key issues in these reanalyses. Results achieved with the selected reanalysis (GLORYS-free) through the downscaling approach show a very good match to high resolution purse seine catch data in the main fishing ground. Skipjack dynamics in both coarse and high resolutoin simulations are close and coherent. Together they allowed to describe the strengh of connectivity links between proposed regions. Connectivity has been highlighted between equatorial region and North Pacific region through the western boundary current system and the central Pacific region. However the simulations do not indicate at this stage a strong impact of equatorial fisheries on the north Pacific skipjack stock, because of a quite high biomass predicted in the equatorial regions exploited by the purse seiners.

Currently SEAPODYM includes several fixed parameters defining the structure of the population and that generate some uncertainty on the model results. Those parameters are defining growth

(weight and size at age) and age at maturity, and are currently derived from MULTIFAN-CL estimates or the literature. Growth and age at maturity are directly observable and usually well defined from biological studies and estimated from statistical approaches. Ideally, they should be estimated directly with the other parameters of SEAPODYM. This is an objective for further developments in the code of the model. An alternative would be to investigate the sensitivity around these parameters in a biologically reasonable range of values. However, for each value tested parameter optimization experiments should be used, and then the best solution selected on the basis of classical statistical metrics. However, given the computational cost associated to parameter optimisation, the range of values should be limited, e.g., to min-max values per parameter.

One more source of uncertainty exists for the high resolution skipjack simulation that comes from its parameterization derived from the coarse INTERIM optimization and not through a direct optimization experiment. Unfortunately, the computational requirement is too high currently to run optimization experiment at a resolution of 0.25°. It is possible that with the improved representation of skipjack distribution in the main fishing grounds in the equatorial, the better match between high catch and high concentration of fish would allow the model to predict the catch correctly with a lower biomass in regions 2 ; 3 and 5. In that case, given the connectivity links identified in this study, the impact of purse seine fishing on the adjacent regions and the North Pacific in particular would be higher.

On the other side, there are some indications that interannual environmental variability could be responsible of a decrease in immature and adult stocks in the recent years while higher recruitment would have occured very recently in concordance with favourable conditions associated to El Nino. Unfortunately the selected reanalysis GLORYS-free was available only for the period 2006-2015. It would have been vey useful to extend the analysis at least back to the early 2000 to examine the long term change in the oceanographic conditions and skipjack dynamics in the North Pacific. This should become possible in the coming months with the future release of the new version of GLORYS that, partly due to the feedback of this study, should include data assimilation only outside of the equatorial band. Then, an alternative to the optimization experiment with this high resolution ocean forcing could be a sensitivity analysis searching for the minimum biomass that is sufficient to sustain the current fisheries. This could be achieved by successive decrease of the recruitment coefficient of the Beverton and Holt function.

6. References

Bessières, L., M.H. Rio, C. Dufau, C. Boone, M.I. Pujol, 2012: Ocean state indicators from MyOcean altimeter products, Ocean Sciences, doi:10.5194/osd-9-2081-2012

Dragon AC, Senina I., Conchon A., Titaud O., Arrizabalaga H. and Lehodey P. (2015). Modeling spatial population dynamics of North Atlantic Albacore tuna under the influence of both fishing and climate variability. *Canadian Journal of Fisheries and Aquatic Sciences*, 72(6): 864-878

Ganachaud, A., et al. (2014), The Southwest Pacific Ocean circulation and climate experiment (SPICE),J.Geophys. Res. Oceans,119, doi:10.1002/2013JC009678.

Gordon, A. L., P. Flament, C. Villanoy, and L. Centurioni (2014), The nascent Kuroshio of Lamon Bay, J. Geophys. Res.Oceans, 119, 4251–4263, doi:10.1002/2014JC009882

Hsin, Y.-C., C.-R. Wu, and P.-T. Shaw (2008), Spatial and temporal variations of the Kuroshio east of Taiwan, 1982 – 2005: A numerical study,J. Geophys. Res.,113, C04002, doi:10.1029/2007JC004485

Kim, Y. Y., T. Qu, T. Jensen, T. Miyama, H. Mitsudera, H.-W. Kang, and A. Ishida (2004), Seasonal and interannual variations of the North Equatorial Current bifurcation in a high resolution OGCM, J. Geophys. Res., 109, C03040, doi:10.1029/2003JC002013.

Kiyofuji H. (2016). Skipjack catch per unit effort (CPUE) in the WCPO from the Japanese pole-and-line fisheries. 12th SC WCPFC, Bali, Indonesia 3-11August 2016, WCPFC-SC12-2016/ SA-WP-05, 17 pp.

Lehodey P., (2004) A Spatial Ecosystem And Populations Dynamics Model (SEAPODYM) for tuna and associated oceanic top-predator species: Part II – Tuna populations and fisheries. 17th meeting of the Standing Committee on Tuna and Billfish, Majuro, Republic of Marshall Islands, 9-18 Aug. 2004, Oceanic Fisheries Programme, Secretariat of the Pacific Community, Noumea, New Caledonia, *Working Paper*: ECO-2: 36 pp.

Lehodey P., (2005). Reference manual for the Spatial Ecosystem And Populations Dynamics Model SEAPODYM. First meeting of the Scientific Committee of the Western and Central Pacific Fisheries Commission WCPFC-SC1, Noumea, New Caledonia, 8-19 August 2005. ME IP–1: 54 pp.

Lehodey P., Bertignac M., Hampton J., Lewis T., Picaut J., (1997). El Niño Southern Oscillation and Tuna in the western Pacific. Nature, 389: 715-718

Lehodey P., Chai F., Hampton J. (2003). Modelling climate-related variability of tuna populations from a coupled ocean-biogeochemical-populations dynamics model. *Fisheries Oceanography*, 12(4): 483-494

Lehodey P., Senina I., (2009). A user manual for SEAPODYM version 2.0: application with data assimilation. Fifth regular session of the Scientific Committee of the Western and Central Pacific Fisheries Commission, 10–21 August 2009, Port Vila, Vanuatu, WCPFC-SC5-2009/ EB-IP-13, 82 pp.

Lehodey P., Senina I., Calmettes B, Hampton J, Nicol S. (2013). Modelling the impact of climate change on Pacific skipjack tuna population and fisheries. *Climatic Change,* DOI 10.1007/s10584-012-0595-1, 119 (1): 95-109.

Lehodey P., Senina I., Calmettes B., Hampton J., Nicol S., Williams P., Jurado Molina J., Ogura M., Kiyofuji H., Okamoto S. (2011). SEAPODYM working progress and applications to Pacific skipjack tuna population and fisheries. 7th regular session of the Scientific Steering Committee, 8-17 August 2011, Pohnpei, Federate States of Micronesia. WCPFC-SC7-2011/EB- WP 06. http://www.wcpfc.int/meetings/2011/7th-regular-session-scientific-committee

Lehodey P., Senina I., Murtugudde R. (2008). A Spatial Ecosystem And Populations Dynamics Model (SEAPODYM) - Modelling of tuna and tuna-like populations. Progress in Oceanography, 78: 304-318.

Lehodey P., Senina I., Titaud O., Calmettes B., Conchon A., Dragon A-C., Nicol S., Caillot S., Hampton J, Williams P. (2014). Project 62: SEAPODYM applications in WCPO. 10th regular session of the Scientific Steering Committee, 6-14 August 2014, Majuro, Republic of the Marshall islands. WCPFC-SC10-2014/EB-WP-02 Rev 1.

Pilling G.M., et al. (2016). Examination of trends in abundance of skipjack tuna with an emphasis on temperate Waters. 11th regular Session of the Scinetific Committee of the WCPFC, Pohnpei, Federated States of Micronesia, 5-13 August 2015, WCPFC-SC11-2015/SA-WP-05.

Qiu, B., and R. Lukas (1996), Seasonal and interannual variability of the North Equatorial Current, Mindanao Current, and the Kuroshio along the Pacific western boundary, J. Geophys. Res.,101(C5), 12,315–12,330

Qiu, B., D. L. Rudnick, S. Chen, and Y. Kashino, 2013: Quasi-stationary North Equatorial Undercurrent jets across the tropical north Pacific ocean. Geophysical Research Letters, doi:10.1002/grl.50394.

Qu, T., H. Mitsudera, and T. Yamagata (1998), On the western boundary currents in the Philippine Sea, J. Geophys. Res.,103 (C4), 7537–7548

Senina I., Lehodey P., Calmettes B., Nicol S., Caillot S., Hampton J. and P. Williams (2016). Predicting skipjack tuna dynamics and effects of climate change using SEAPODYM with fishing and tagging data. WCPFC, 12th Regular Session of the Scientific Committee, Bali, Indonesia 3–11 August 2016, WCPFC-SC12-2016/EB WP-01: 71 pp.

Senina I., Sibert J., & Lehodey P. (2008). Parameter estimation for basin-scale ecosystem-linked population models of large pelagic predators: application to skipjack tuna. Progress in Oceanography ,78: 319-335.

Sibert J, Senina I, Lehodey P, Hampton J (2012). Shifting from marine reserves to maritime zoning for conservation of Pacific bigeye tuna (*Thunnus obesus*). *Proceedings of the National Academy of Sciences* 109(44): 18221-18225.

Tranchant B., Reffray G., Greiner E., Nugroho D., Koch Larrouy Ariane, Gaspar P. (2016). Evaluation of an operational ocean model configuration at 1/12 degrees spatial resolution for the Indonesian seas (NEMO2.3/INDO12) : Part 1 : Ocean physics. Geoscientific Model Development, 9 (3), p. 1037-1064.

WCPFC (2016). Summary Report. Scientific Committee Twelfth Regular Session Bali, Indonesia 3-11 August 2016.

Williams P., Terawasi (2016). Overview of tuna fisheries in the Western and Central Pacific Ocean, including economic conditions - 2015 Rev 3 (15 July 2016).

7. Appendix

7.1. Table A1: Fisheries

Definition of fisheries and fishing data used in basin scale optimization experiments performed for Pacific Ocean domain.

ID	Description	Nation	Resolution	Time period
P1	Sub-tropical pole-and-line	Japan	1°, month	1972 - 2012
P21	Pole-and-line	Japan	1°, month	1972 - 1982
P22	Pole-and-line	Japan	1°, month	1982 - 1990
P23	Pole-and-line	Japan	1°, month	1990 - 2012
P3	Tropical pole-and-line	Pacific Islands	1°, month	1970 - 2012
S4	Sub-tropical purse-seine	Japan	1°, month	1970 - 2012
S5	PS anchored FADs, WCPO	ALL	1°, month	1967 - 2012
S6	Purse-seine	Philippines, Indonesia	1°, month	1986 - 2010
S7	PS free schools, WCPO	ALL	1°, month	1967 - 2012
L8	Longline, WCPO	ALL	5°, month	1950 - 2012
L9	Longline, Domestic fisheries	Philippines, Indonesia	5°, month	1970 - 2011
S10	PS FADs, EPO	ALL	1°, month	1996 - 2013
S11	PS LOGs, EPO	ALL	1°, month	1996 - 2013
S12	PS Animal associations, EPO	ALL	1°, month	1996 - 2013
S13	PS Free schools, EPO	ALL	1°, month	1996 - 2013
S14	PS Unknown log, EPO	ALL	1°, month	1996 - 2013
P15	Pole-end-line, EPO	ALL	5°, month	1972 - 2008
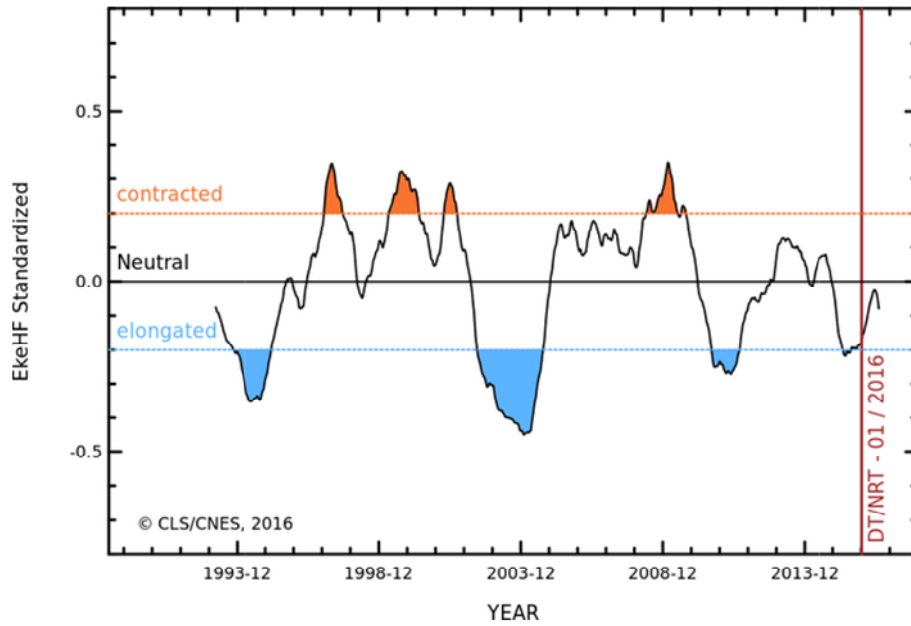
7.2. Figure A1: Kuroshio state

Standardized Eddy Kinetic Energy (EKE) over the Kuroshio region. Blue shaded areas correspond to elongated states periods (1993-94, 2002-04 and 2010-11), while orange shaded areas fit contracted states periods (1997-2001 and 2009).
https://www.aviso.altimetry.fr/en/data/products/ocean-indicators-products/kuroshio.html
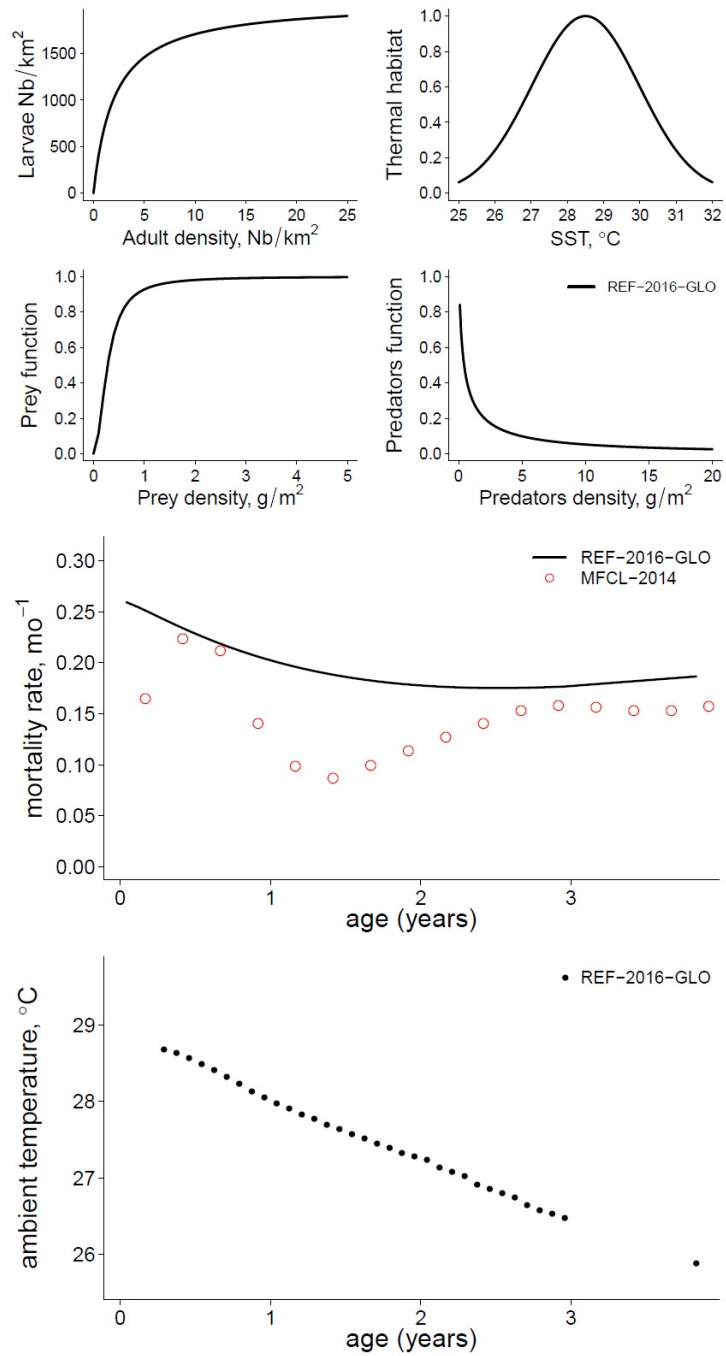
7.3. Figure A2: Functional relationships

Estimated parameters in the INTERIM skipjack optimization experiment based on catch, length frequencies and tagging data. Evolution of main model parameters through population life history: (from top to bottom) - reproduction functions, average mortality rates and preferred habitat temperature.
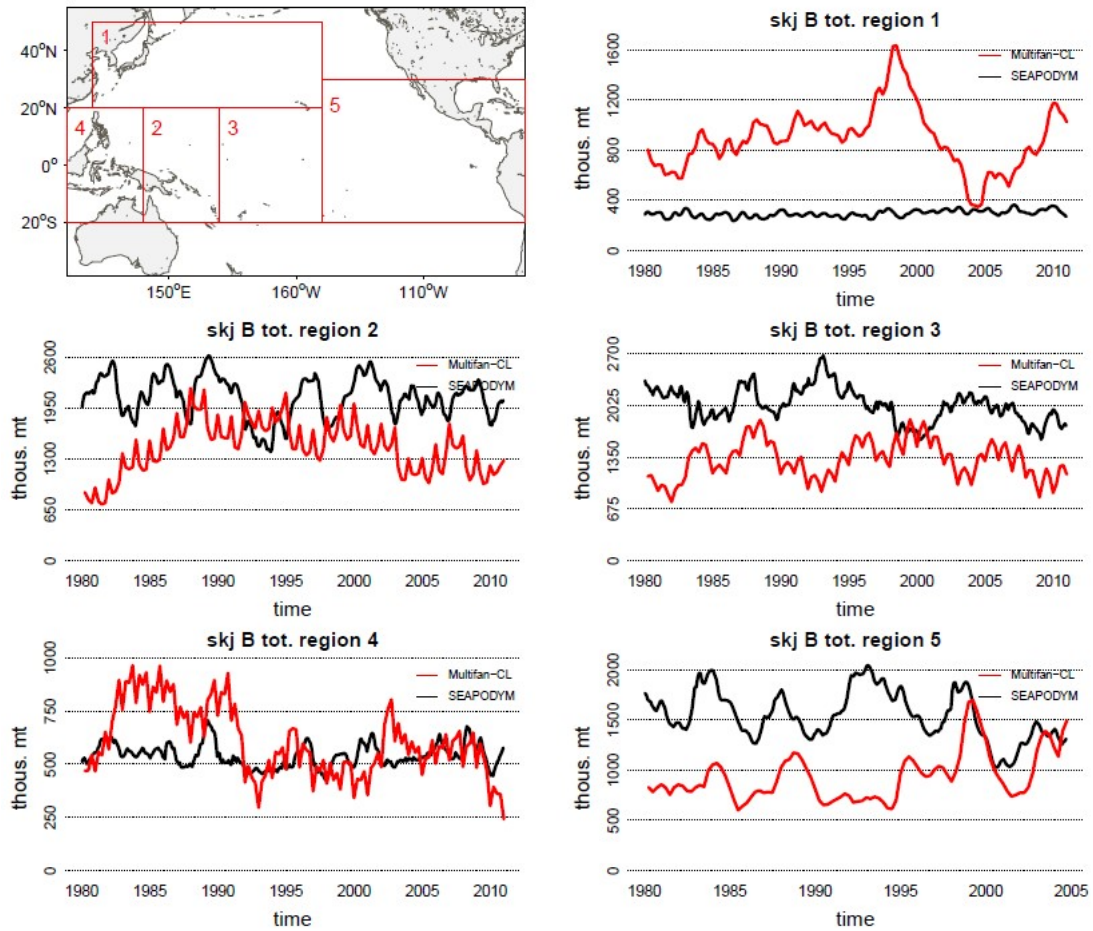
7.4. Figure A3: INTERIM SEAPODYM vs MFCL

Regional comparison between SEAPODYM and Multifan-CL model predictions for total (immature and mature) biomass. Reference INTERIM simulation is shown by solid black line and MULTIFAN-CL by red line.(From Senina et al 2016)
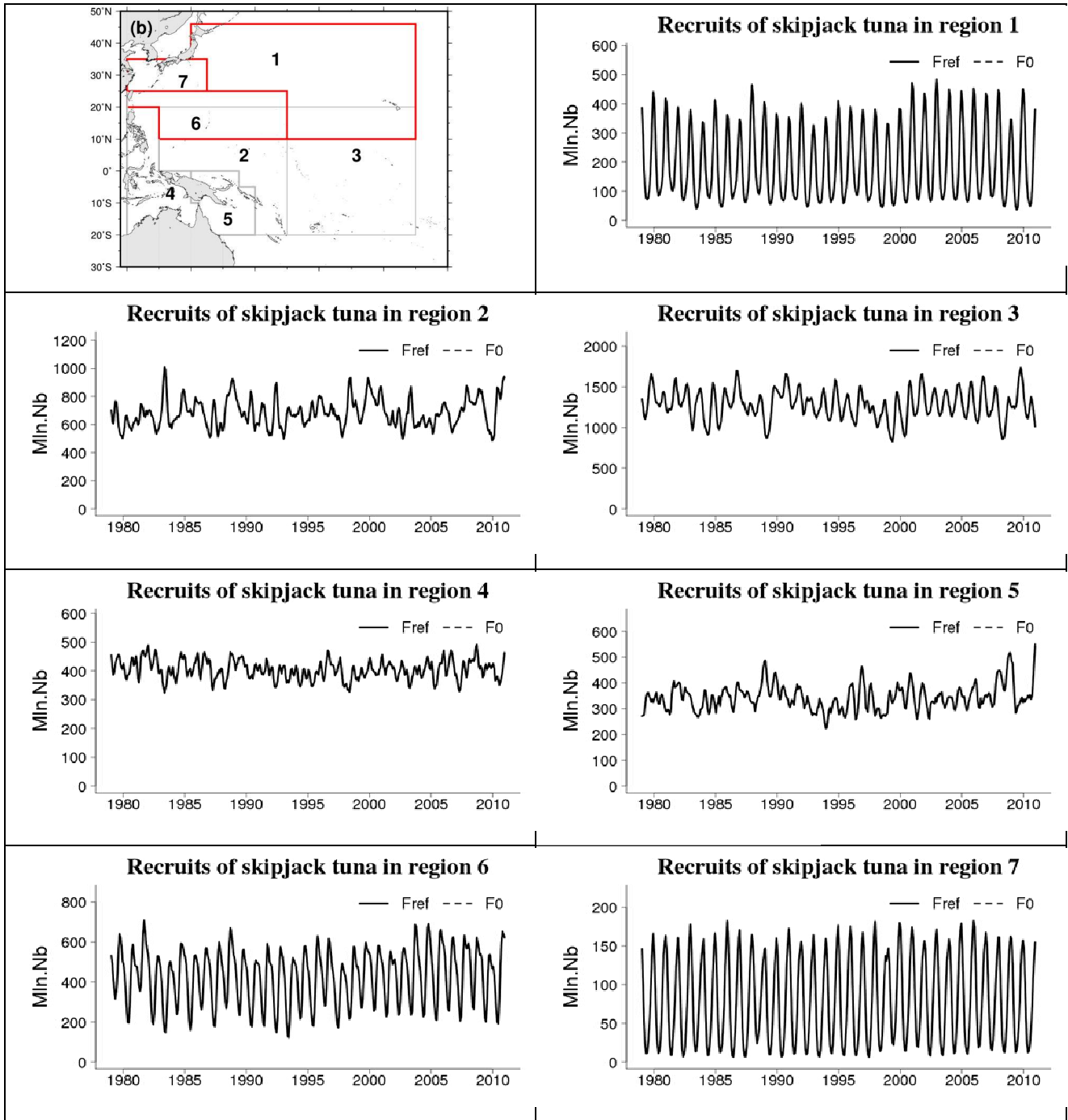
7.5. Figure A4: Recruits by region

Predicted biomass of recruits (in numbers) by region based on regions defined in Hidetada (2016) using INTERIM reference simulation.
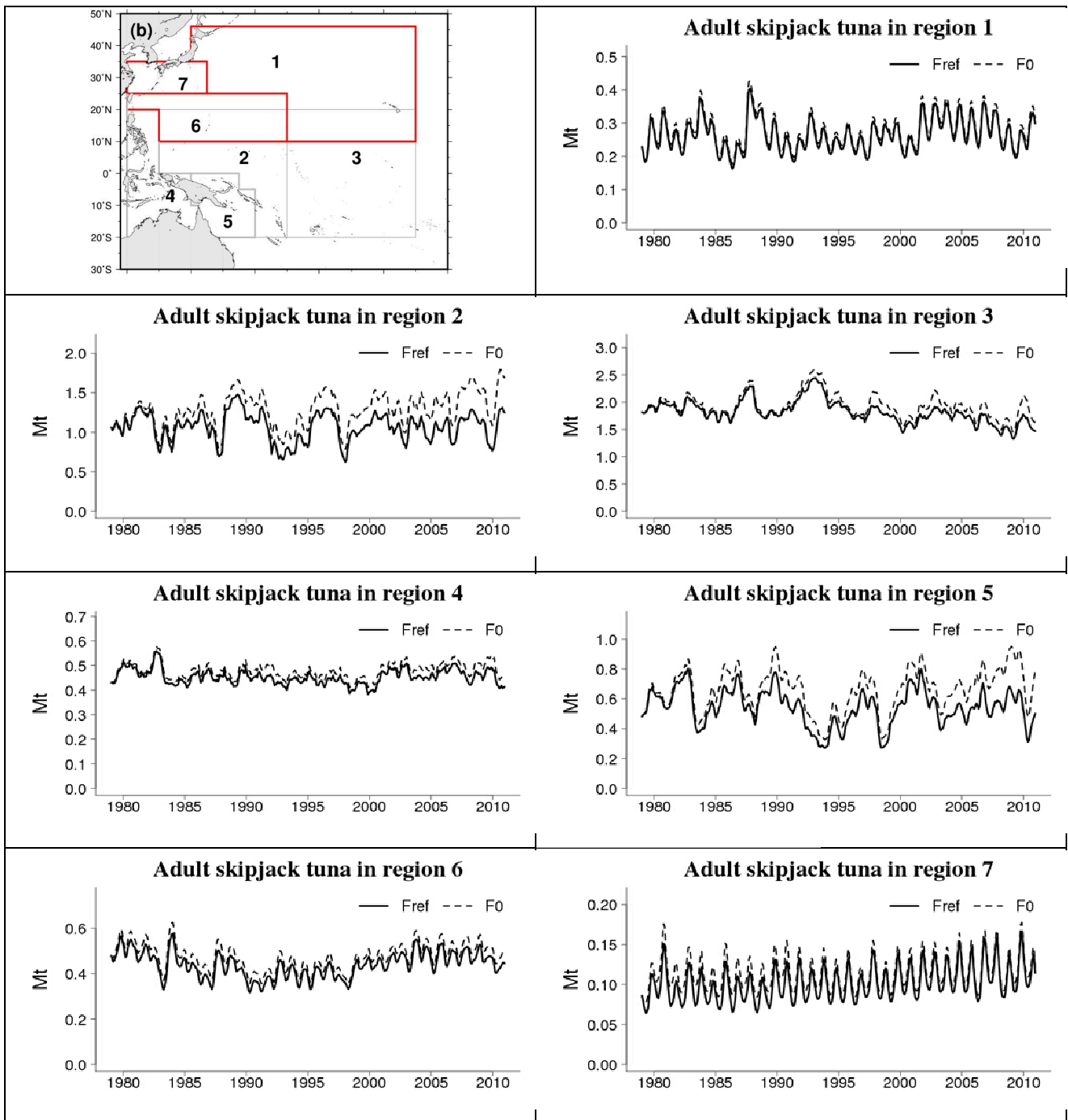
7.6. Figure A5: Adult SKJ by region

Predicted biomass of adults (in metric tonnes) by region based on region defined in Kiyofuji (2016) using INTERIM reference simulation.
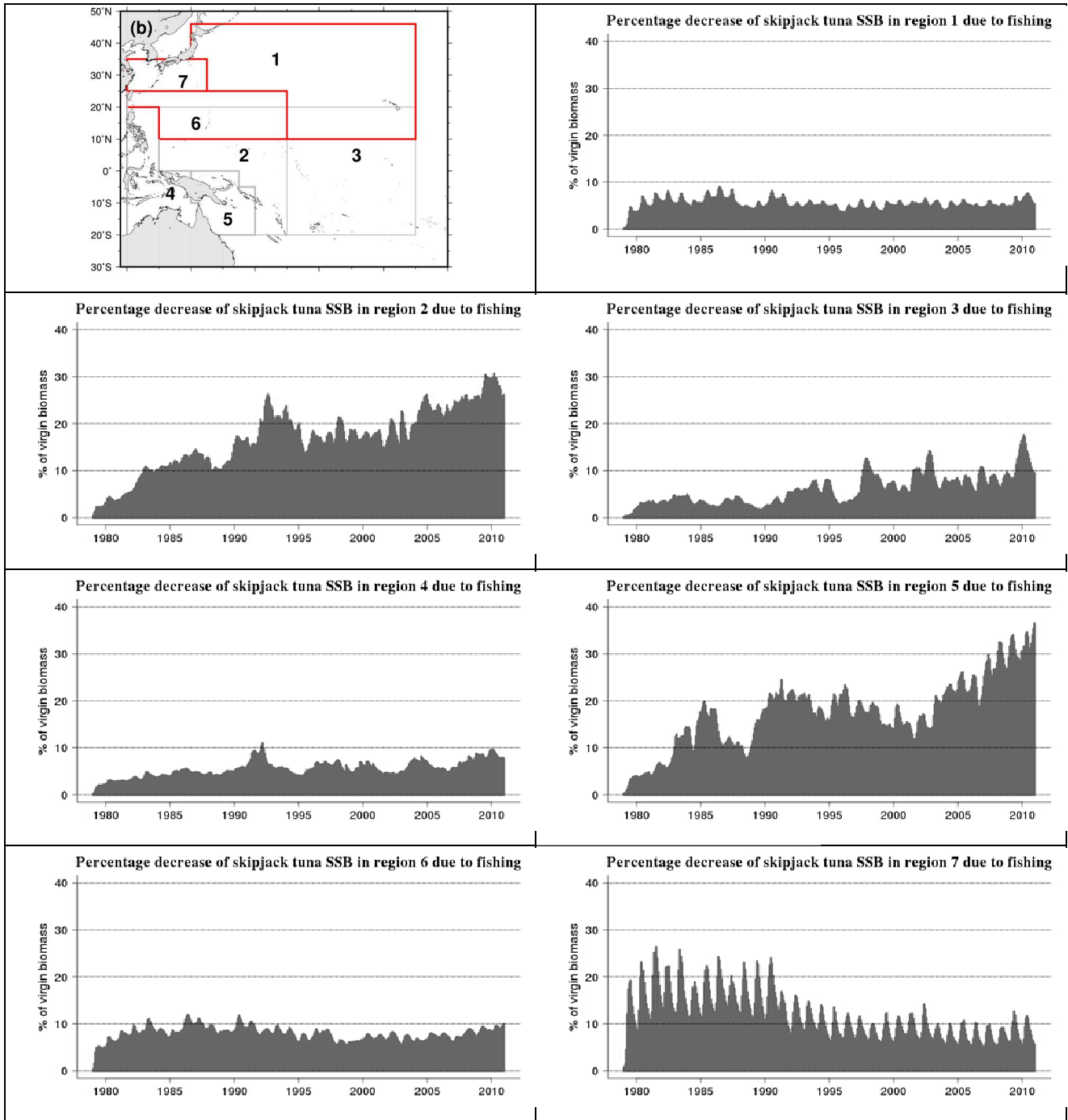
7.7.   Figure A6: Fishing impact by region

Predicted impact of fishing on adult (spawning) biomass by region based on region defined in
Kiyofuji (2016) using INTERIM reference simulation.

RSGFt

R−squared goodness of fit (Total catch over 2006/1 − 2015/12)
mean=0.56, nbc.pos=175

R²

Pearson R−squared (Total catch over 2006/1 − 2015/12)
mean=0.73, nbc.pos=241
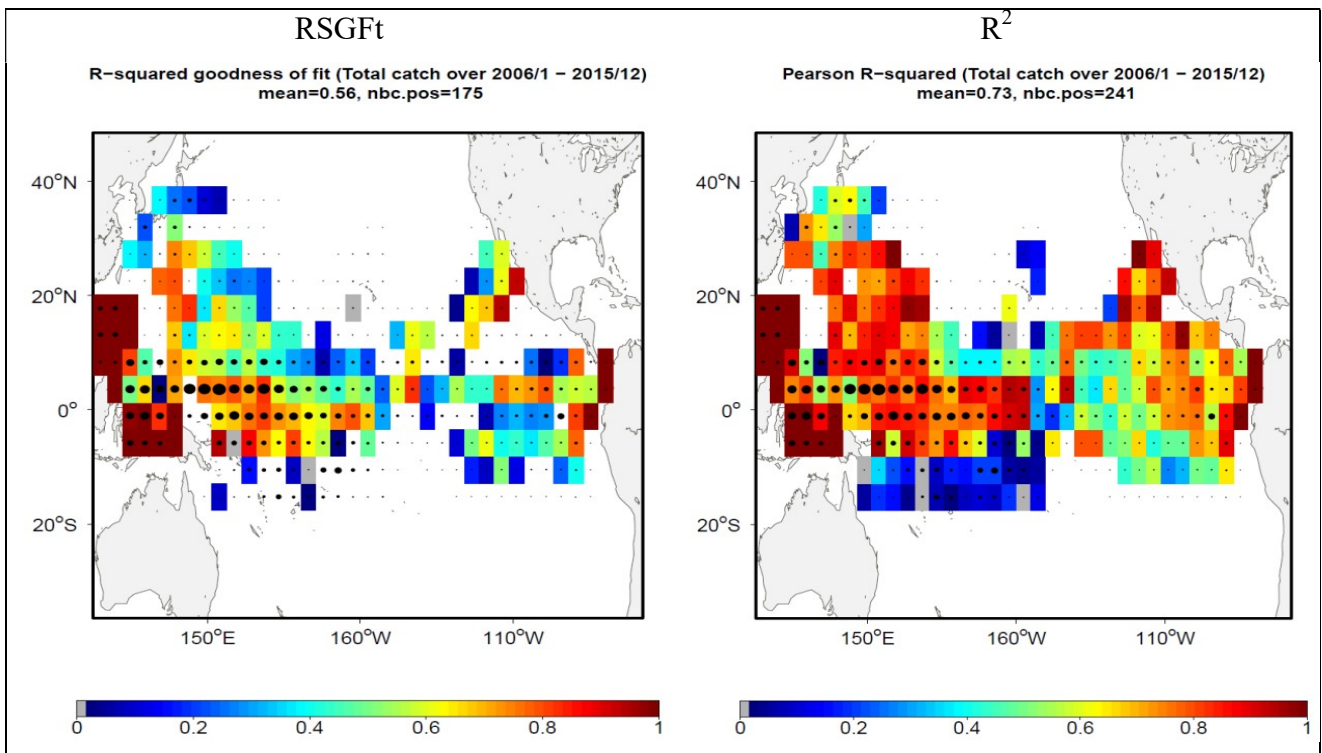
7.8. Figure A7: Overall fit to catch data (GLORYS)

Fit to fishing data over all the period 2006-2015: R-squared goodness of fit, and squared Pearson correlation coefficient; black circles are proportional to the level of catch.

The RSGF (standard R-squared goodness of fit) gives a measure of fit to absolute values of catch for all the fleets over the whole simulation period. It can vary between $-\infty$ (no fit) and 1 (perfect fit).

The squared Pearson correlation coefficient (R^2) between time series of predicted and observed data in each spatial cell provides a metric on the model skills for predicting the variability (e.g., seasonal and interannual fluctuations) in the data.

7.9. Figure A8: GLORYS2v4 SKJ distribution and catch at ¼°x week
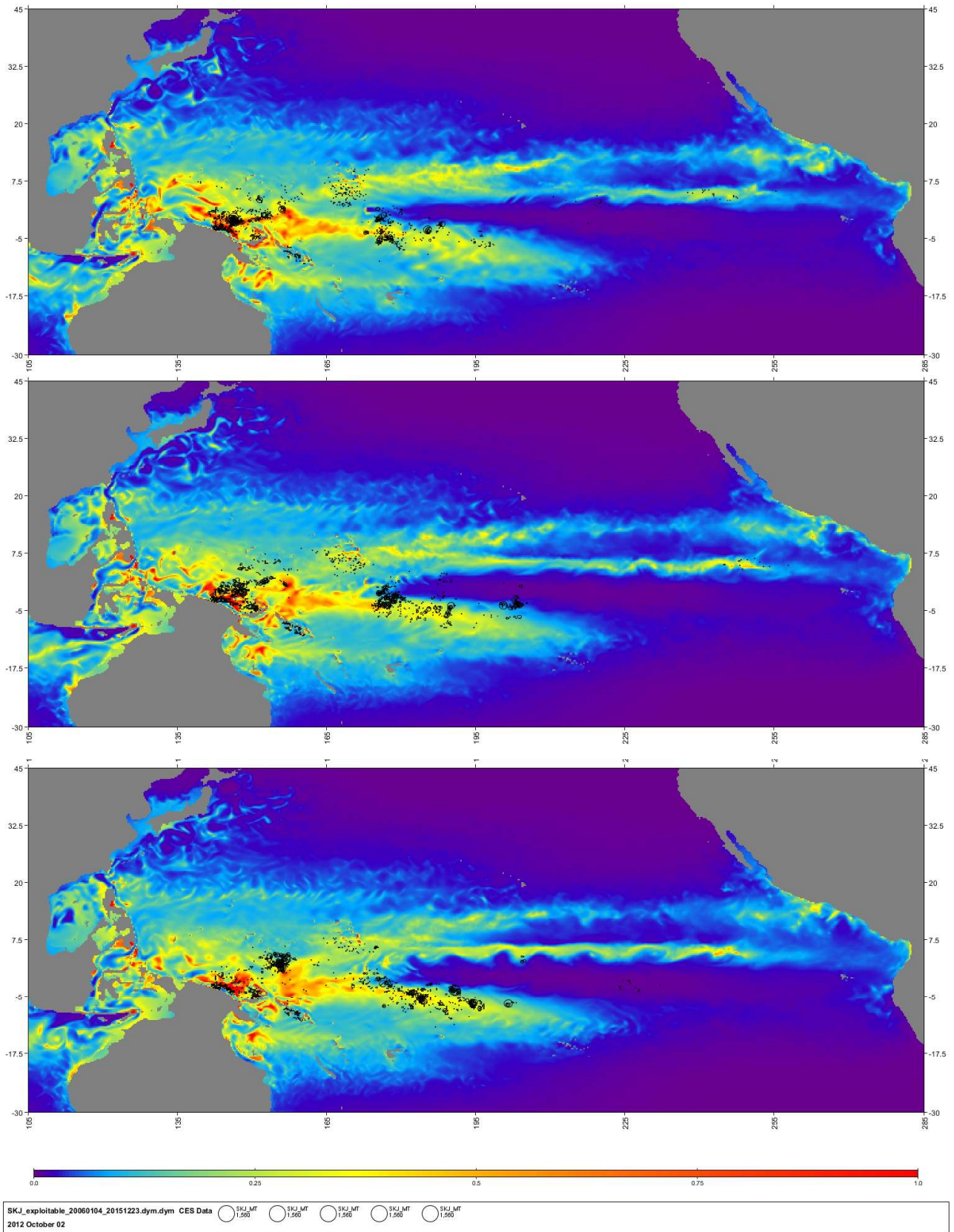
Weekly distributions of skipjack (exploitable biomass 30-70 cm) in 2012 and monthly catch of purse seine fisheries
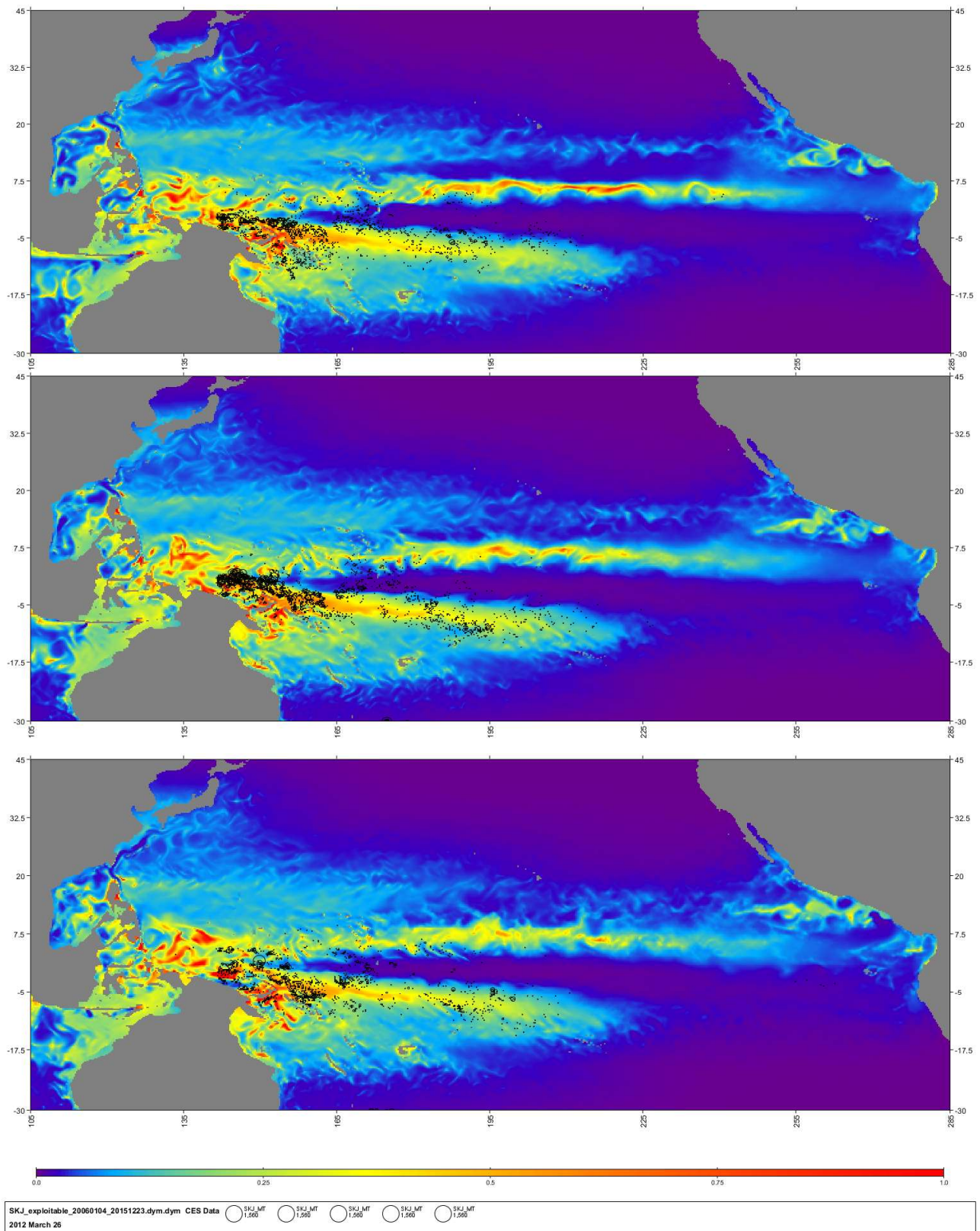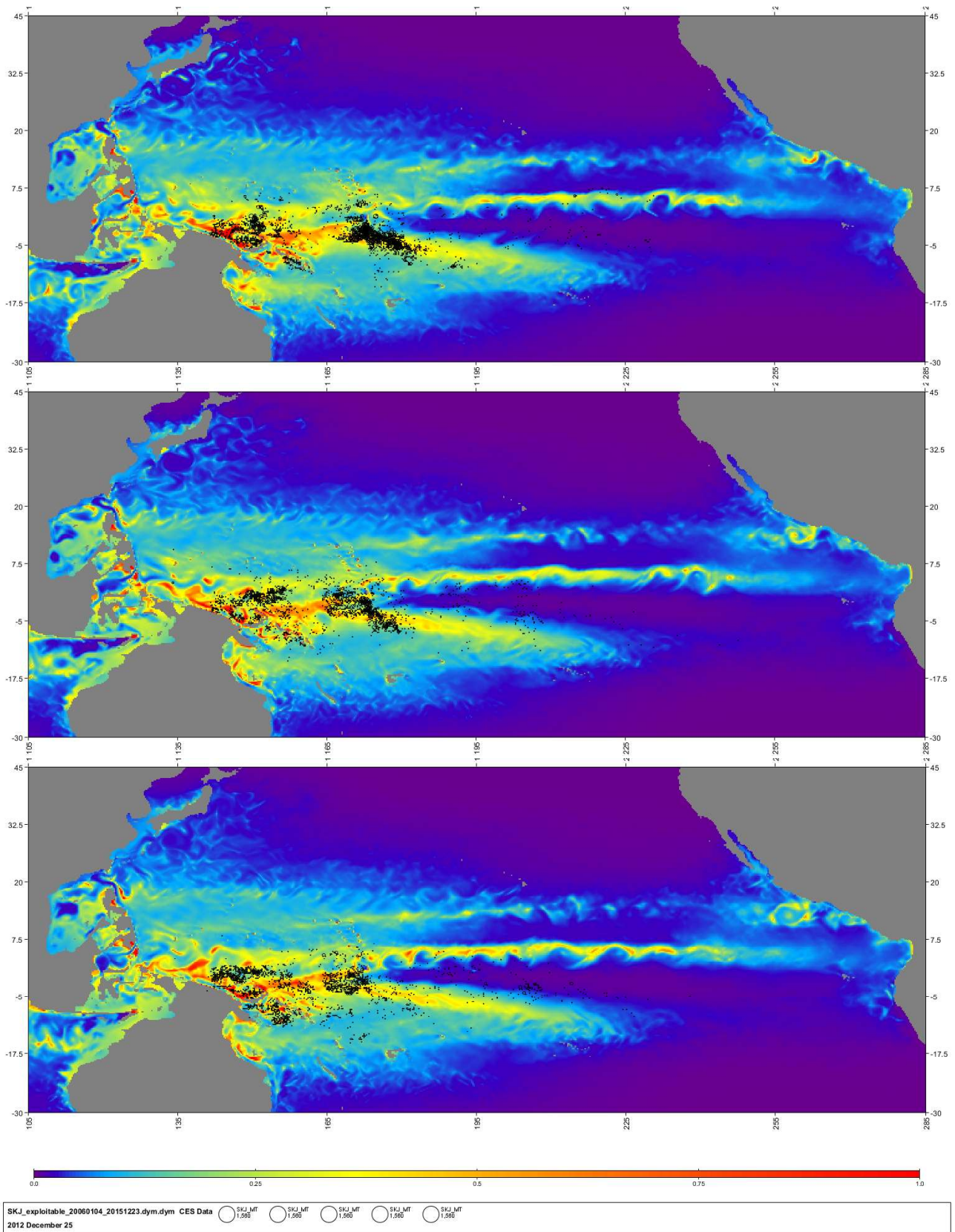

Weeks starting on Jan 04, Feb 14 and Mar 26 with monthly catch
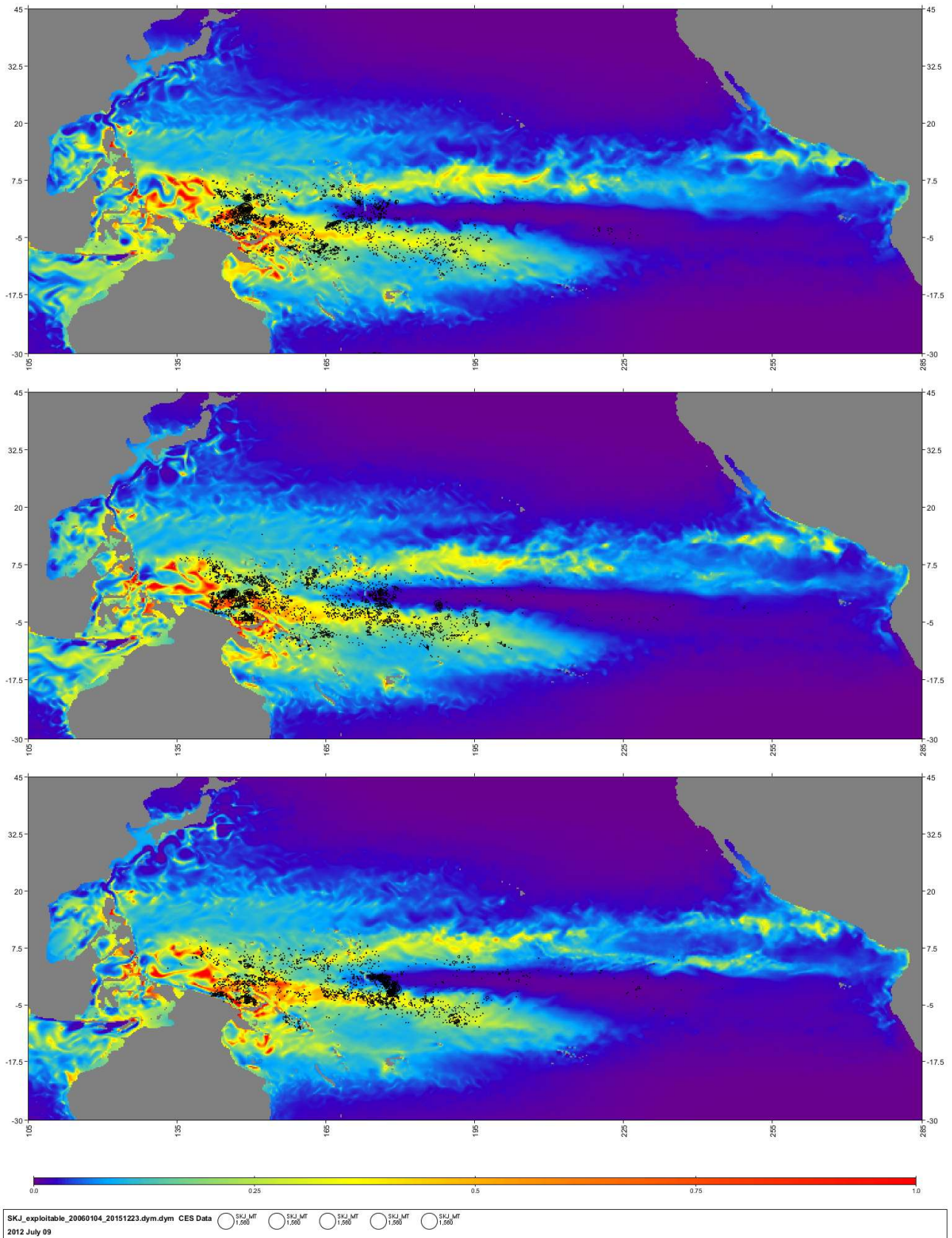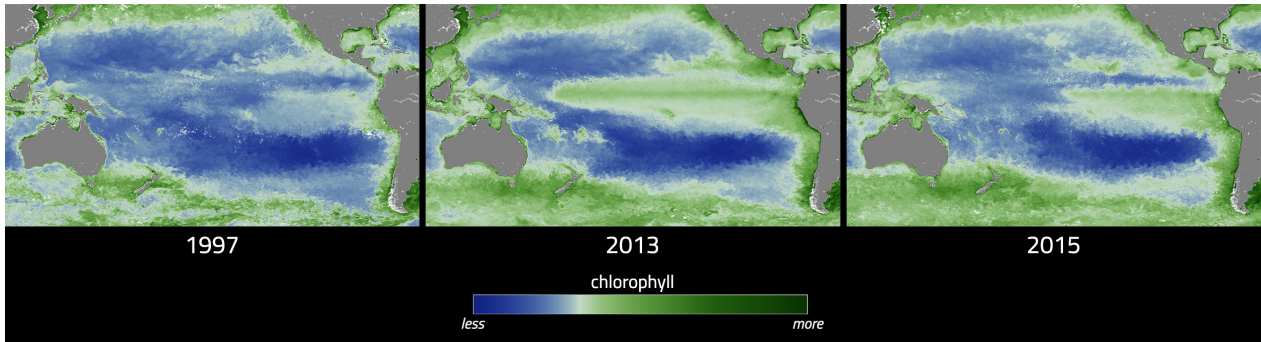
Weeks starting on Apr 30, Jun 04 and Jul 09 with monthly catch

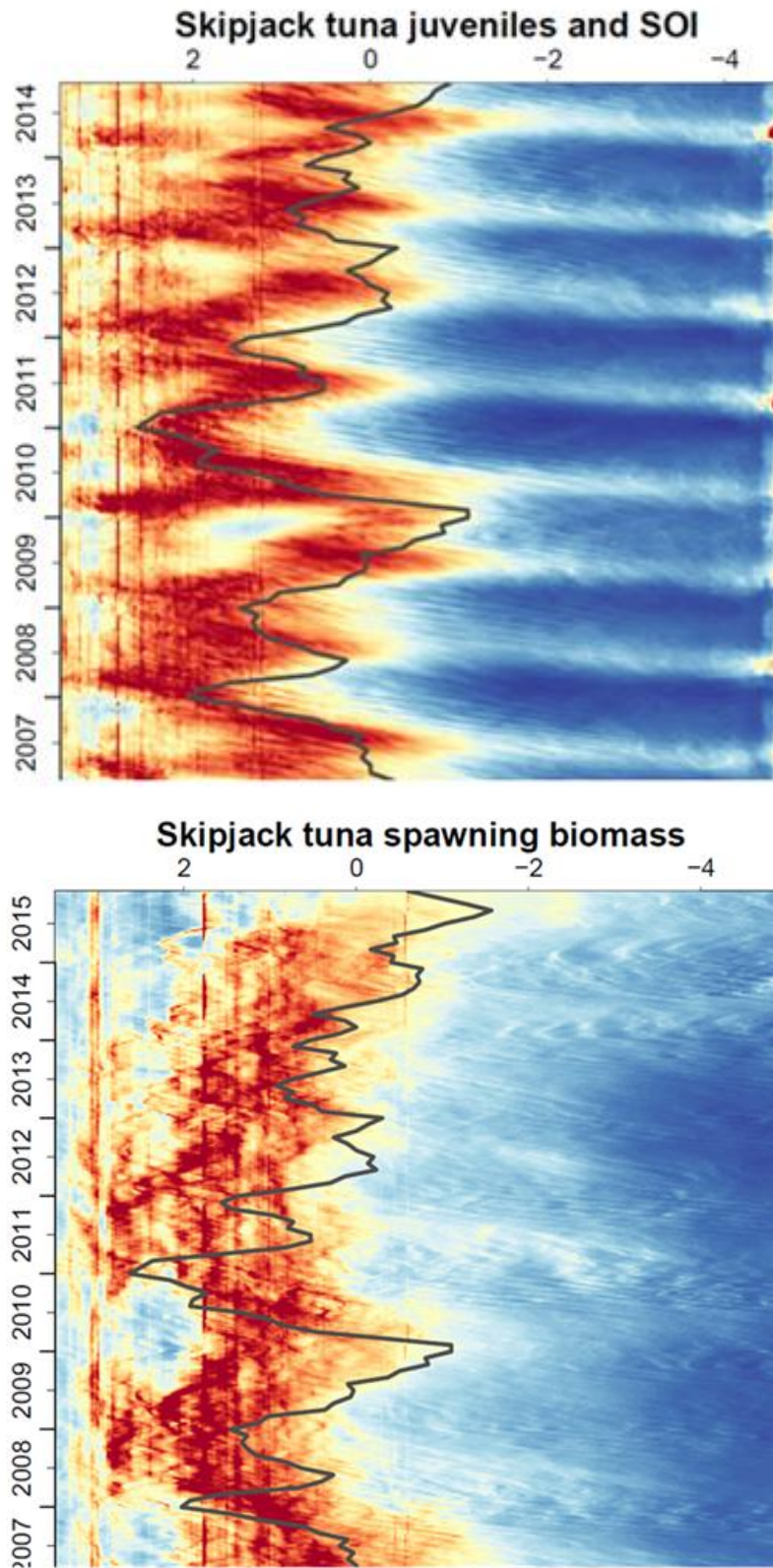Weeks starting on Aug 06, Sep 04 and Oct 02 with monthly catch

Weeks starting on Oct23, Nov 27 and Dec 25 with monthly catch

7.10. Figure A9: ENSO Modoki (Figure to be updated)

Annual mean satellite derived chlorophyll concentration during El Nino event of 1997, La Nina event of 2013 and El Nino-Modoki event of 2015. Credits: Uz/NASA Goddard

7.11. Figure A10: ENSO and skipjack

Hovmöller time-longitude plots of juveniles and adult (spawning) skipjack biomass averaged in the 10°N-10°S latitudinal band.